Final Report for the

LOW EARTH ORBIT RAIDER (LER)

WINGED AIR LAUNCH VEHICLE CONCEPT

NASW-4435

A design project by students in the Department of Aerospace Engineering at Auburn University under the sponsorship of the NASA/USRA University Advanced Design Program.

Auburn University

Auburn University, Alabama

June 1989

. . . Continuing Education is Essential . . .

Aerospace Engineering Department

Auburn University

Auburn University, Alabama

Low Earth Orbit Raider

(LER)

Winged Air Launch Vehicle Concept

Volume 1: Design

Submitted to: Dr. James O. Nichols

Submitted by: Karl Feaux

William Jordan

Graham Killough

Robert Miller

Vonn Plunk

Date Submitted: May 4, 1989

ABSTRACT

The need to launch small payloads into low earth orbit has increased dramatically during the past several years. The Low Earth orbit Raider (LER) is an answer to this need.

The LER is an air-launched, winged vehicle designed to carry a 1500 pound payload into a 250 nautical mile orbit. The LER is launched from the back of a 747-100B at 35,000 feet and a Mach number of 0.8. Three staged solid propellant motors offer safe ground and flight handling, reliable operation, and decreased fabrication cost. The wing provides lift for 747 separation and during the first stage burn. Also, aerodynamic controls are provided to simplify first stage maneuvers.

The air-launch concept offers many advantages to the consumer compared to conventional methods. Launching at 35,000 feet lowers atmospheric drag and other loads on the vehicle considerably. Since the 747 is a mobile launch pad, flexibility in orbit selection and launch time is unparalleled. Even polar orbits are accessible with a decreased payload. Most importantly, the LER launch service can come to the customer, satellites and experiments need not be transported to ground based launch facilities.

The LER is designed to offer increased consumer freedom at a lower cost over existing launch systems. Simplistic design emphasizing reliability at low cost will allow the LER to be the industry leader in light payloads for years.

TABLE OF CONTENTS

ABSTRACT ii

LIST OF FIGURES iv

LIST OF TABLES v

LIST OF SYMBOLS vi

INTRODUCTION 1

VEHICLE DESCRIPTION 4

TECHNICAL ANALYSIS 8

- Mission Trajectory 8
- Aerodynamics 14
- Propulsion 26
- Materials 43
- Structures 48

DEVELOPMENT TIMETABLE 51

DEVELOPMENT COST SUMMARY 55

SUMMARY AND RECOMMENDATIONS 58

REFERENCES 60

LIST OF FIGURES

Number	Title	Page
1	The LER - Not to Scale	3
2	Three Dimensional View of the LER	5
3	Schematic of the LER Trajectory	9
4	Altitude and Velocity vs Time for the LER Ascent	13
5	Skin Friction Coefficient verses Reynold's number for Incompressible Flow	15
6	Laminar/Turbulent Flow Transition Point	16
7	Lift and Drag versus Altitude for LER Ascent	25
8	Cross Sectional View of 3-Point Grain Design	27
9	Circumference vs Regression for LER Motors	29
10	Thrust and Pressure vs Time for the First Stage Motor	39
11	Thrust and Pressure vs Time for the Second Stage Motor	40
12	Thrust and Pressure vs Time for the Third Stage Motor	41
13	Movable Nozzle Design for Second and Third Stage Motors	42
14	Costs of Common Engineering Materials per Cubic Inch	45
15	Fabrication of Solid Rocket Casing	47
16	Solid Rocket Motor Structurals	49
17	Composite Wing Design Options	50
18	LER Development Timetable	52

LIST OF SYMBOLS

Symbol	Description	Units
Ab	Propellant burn rate	in^2
Ac	Cross sectional area of casing	in^2
Ae	Nozzle exit area	in^2
Aopen	Cross sectional area of open space in combustion chamber	in^2
Aprop	Cross sectional area of propellant	in^2
AR	Aspect Ratio	--
A*	Nozzle throat area	in^2
a	Burning rate coefficient	--
b	Wing span	ft
C_D	Drag coefficient	--
C_{Df}	Coefficient of drag due to friction	--
C_{Di}	Incidence drag coefficient	--
C_{Dp}	Parasite drag coefficient	--
C_{Dw}	Coefficient of wave drag	--
C_{Fl}	Laminar coefficient of friction	--
C_{Ft}	Turbulent coefficient of friction	--
C_L	Coefficient of lift	--
$C_{L\alpha}$	Coefficient of lift with α	--
c	Chord length	ft
c*	Characteristic exhaust velocity	ft/sec
D	Drag	lbf
d	diameter	in,ft
de	Nozzle exit diameter	in,ft
e	Oswald's efficiency factor	--
F	Thrust	lbf

Symbol	Description	Units
Fty	Yield stress in tension	ksi
Ftu	Ultimate stress in tension	ksi
Fcy	Yield stress in compression	ksi
Fsy	Yield shearing stress	ksi
FPA	Flight path angle	degrees
g	Acceleration due to gravity	$\frac{lbm\ ft}{lbf\ s^2}$
h	Altitude	ft,n.mi
Isp	Specific Impulse	sec
L	Lift	lbf
L,l	Length	in,ft
M	Mach number	--
m	mass flow rate	$\frac{lbm}{s^2}$
m	mass	lbm
M	Molecular weight of exhaust gases	$\frac{lbm}{lbm\ mol}$
Me	Nozzle exit mach number	--
n	Propellant burn rate exponent	--
Pc	Combustion pressure	psia
Pe	Nozzle exit pressure	psia
R	Universal gas constant	1545 $\frac{lbm\ ft}{lbm\ mol\ ^\circ R}$
R	Radius of LER	in
r	Casing inner radius	in
r	Casing outer radius	in
Re,Rn	Reynold's number	--
SF	Saftey factor	--

Symbol	Description	Units
Sx	Wetted area over length x	ft^2
Se	Total wetted area	ft^2
Sref	Reference area	ft^2
Swet	Wetted area	ft^2
Tc	Flame temperature	°R
t	time	sec
t	thickness	in
T	thrust	lbf
V	Volume	in,ft
v	velocity	ft/sec
V	Burnout velocity	ft/sec
W	Weight	lbf
α	Angle of attack	degrees
α	Nozzle cone divergence half angle	degrees
θ	Flight path angle	degrees
ν	Kinematic viscosity	ft^2/sec
ρ	Density	lbm/ft^3
σ	Flight path angle	degrees
σ	Ogive semi-vertex angle	degrees
$\sigma_{A(t)}$	Axial stress (tension)	psi
$\sigma_{A(c)}$	Axial stress (compressive)	psi

INTRODUCTION

The need for low cost access to space has increased dramatically over the past few years. With the failure of NASA's Space Shuttle to reliably carry commercial payloads into space, some other method must be found to keep America's companies competitive in the growing space market. Experiments by universities, government agencies, and corporations that were to be carried into space two years ago by NASA are gathering dust. Also, developing nations have a need to send small packages into orbit in an attempt to enter the space age. For these reasons, a low cost launch system is needed to send small satellites and experiments into low earth orbit.

One highly promising method for sending such payloads into low earth orbit is to carry a small, winged, expendable launch vehicle on an airplane to cruise altitude. The launch vehicle will then separate from the host aircraft and carry the satellite or experiment into space. This type of system allows increased flexibility for the consumer over conventional land based launch systems. Also, starting at a high cruise altitude has certain benefits to mission efficiency. These benefits include: lower air pressures, since over 60% of the earth's atmosphere is below launch altitude; lower required structural strength and weight; and a 1-2% increase in total propulsive efficiency due to the

initial velocity. These advantages lead to lower costs per launch.

Therefore, it is proposed to carry such a launch vehicle, known as the Low Earth orbit Raider (LER) (Figure 1), on the back of a Boeing 747. This three stage solid rocket propelled vehicle will be capable of delivering payloads of 600 to 1500 pounds to low earth orbits up to 250 nautical miles. The LER will have a wing so that aerodynamic forces can be used to help lift the system into space. Anticipated cost per launch is around ten million dollars.

Many advantages exist for developing such a launch system. The host 747 can launch the vehicle from any place in the world into any orbit desired, including polar orbits. Since polar orbits are inaccessible by NASA from Cape Canaveral, Florida, this ability would give American launch customers increased flexibility. The 747 may be operated from any airport capable of handling wide-body jets, allowing the LER to come directly to the customer. By building a simple launch vehicle at the lowest cost possible, access to space can be made available to virtually any company or country.

For the past nine months, the LER has undergone intense performance estimates. This report is a culmination of the research and design work accomplished. On the basis of the research, it is believed that the LER system will provide reliable, flexible, low cost launch service to a variety of consumers.

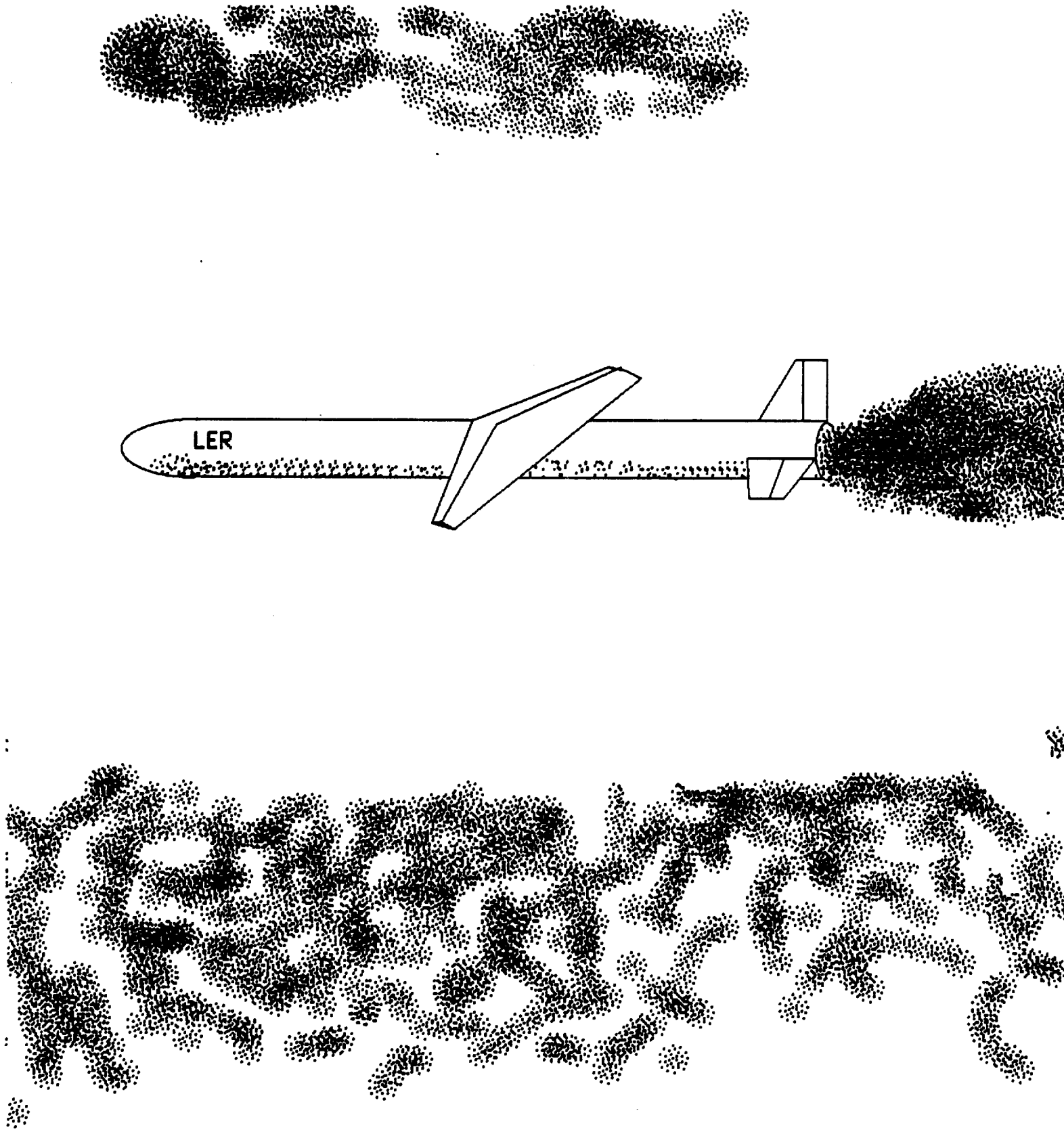

Figure 1. LER-Not to scale.

VEHICLE DESCRIPTION

The basic configuration of the LER is composed of four parts: the nose, body, wing, and tail. This configuration with dimensions is shown in Figure 2. The purpose of this section of the report is to discuss some of the specific aerodynamic and geometric characteristics of each component.

The nose/payload area considered in the LER design is a tangent ogive with a cylindrical volume in the rear. An ogive is a shape formed by an arc rotated about the longitudinal axis of the body. The base of a tangent ogive nose is tangent to the cylindrical mid-section of the body. The ogive nose shape has several advantages over other nose shapes. These advantages are:

1. Greater volume
2. Greater structural integrity
3. Low cost construction.

The radius of curvature of the nose is 75 inches and the payload volume is 92.04 cubic feet.

The LER body is cylindrical is shape. The body is 60 inches in diameter and 660 inches in length. The cylindrical shape is structurally sound, has little drag, and is easily manufactured.

The primary lifting component of the first stage is the wing. The wing is designed to lift the LER from the back of

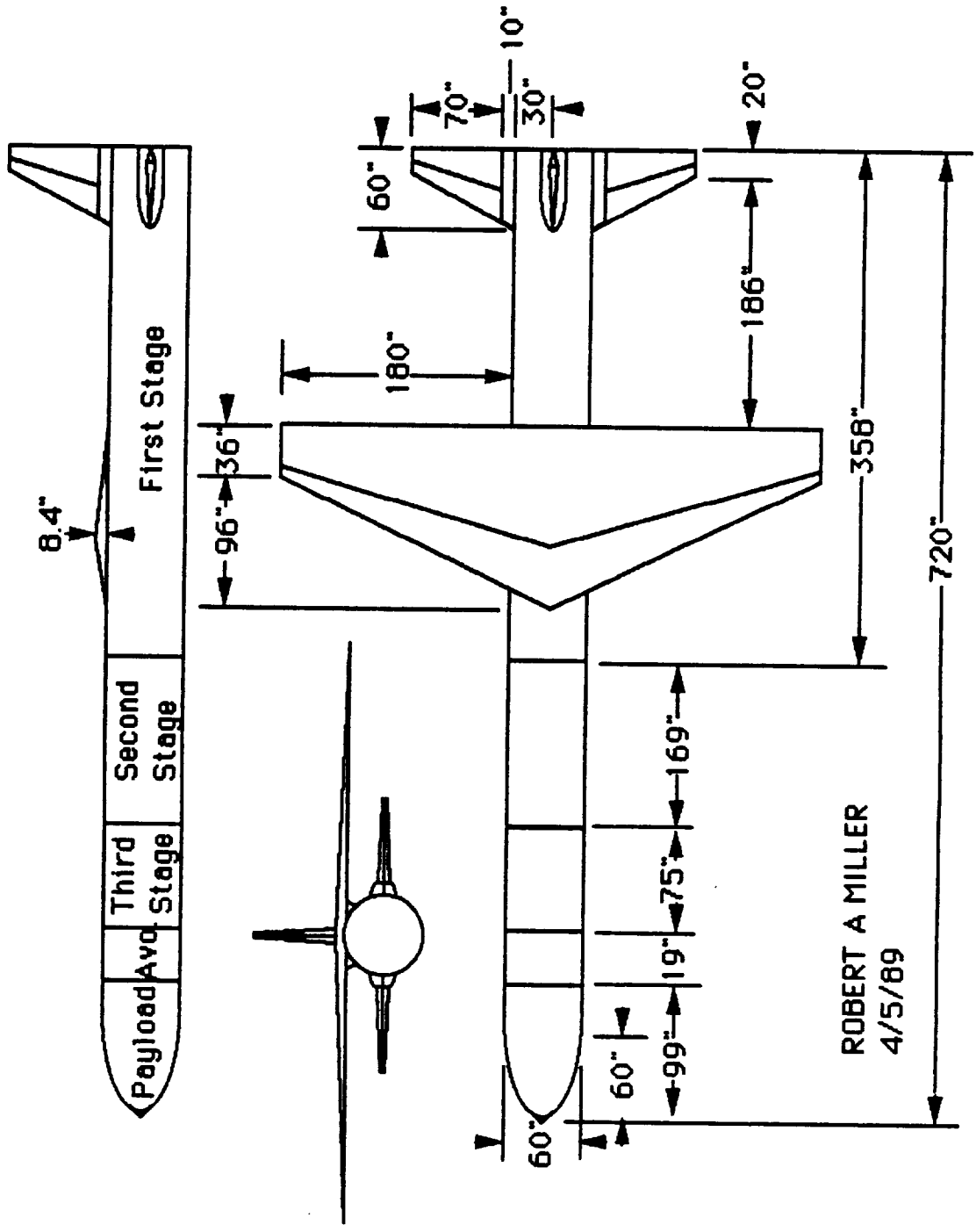

Figure 2: Three Dimensional View of the LER

the 747 during separation. All pertinent wing characteristics are given in Table 1. The LER wing has a fairly high aspect ratio for supersonic flight. A large aspect ratio is used to increase the lift during separation. The wing sweepback angle serves to decrease the wave drag of the wing. The quarter chord of the wing is located at the center of gravity of the LER at launch. As the center of gravity moves forward during flight, stability is enhanced.

The tail section consists of three equally sized, all-moving fins. These fins, built of composites, are lightweight and easy to manufacture. They are of bi-convex design, with the largest thickness occurring at the center of the chord. Table 2 lists all important fin characteristics.

The bulk of the LER weight is made up of the solid propellant. Through the use of advanced composite materials and construction techniques, structure weight is only 6% of the total launch weight. Table 3 lists some of the pertinent weight estimates.

Table 1: Wing Parameters

Item	Value
wing span	35.0 feet
root chord	11.0 feet
tip chord	3.0 feet
taper ratio	0.273
aspect ratio	5.0
sweep angle (leading edge)	25.75 deg
planform area	245 feet^2
wetted area	437.9 feet^2
thickness to chord ratio	7.0%
maximum thickness location	1/4 chord

Table 2: Tail Fin Characteristics

Item	Value
fin span	5.833 feet
root chord	5.0 feet
tip chord	1.67 feet
taper ratio	0.334
sweep angle (leading edge)	29.75 deg
wetted area	36.11 feet^2
thickness to chord ratio	7.0%
maximum thickness location	1/2 chord

Table 3: LER Weight Estimates

Item		Weight
payload		1500 lb
payload fairing		300 lb
avionics and thrusters		130 lb
third stage propellant		5023 lb
third stage structure		556 lb
second stage propellant		13276 lb
second stage structure		719 lb
first stage propellant		37993 lb
first stage structure		1937 lb
	TOTAL	61434 lb

TECHNICAL ANALYSIS

Initial technical analysis and performance estimation has been accomplished for the LER project. The analysis work is broken into several distinct areas; mission profile, aerodynamics, propulsion, materials, and structures. A synopsis of the work performed in each area is presented.

Mission Trajectory

The mission begins once separation from the Boeing 747 is initiated. The mission profile is broken into four phases: separation, first stage boost, second stage boost and coast, and third stage boost/orbital insertion. Figure 3 is a schematic of the events which occur during the ascent of the LER.

Due to the complexity of the problem, detailed separation analysis has not been accomplished at this time. Feasibility studies, however, show that at a 10 degree angle of attack, the LER wing provides the necessary lift to raise the LER from the 747. The angle of attack is achievable by placing the nose of the LER on the front hump of the 747 cockpit. Interference effects between the LER and 747 still must be investigated. It is believed, however, that the separation phase of the mission is not insurmountable.

The boost phases have been fully analyzed, and workable trajectories are attainable. The trajectory calculations include full atmospheric lift and drag until the

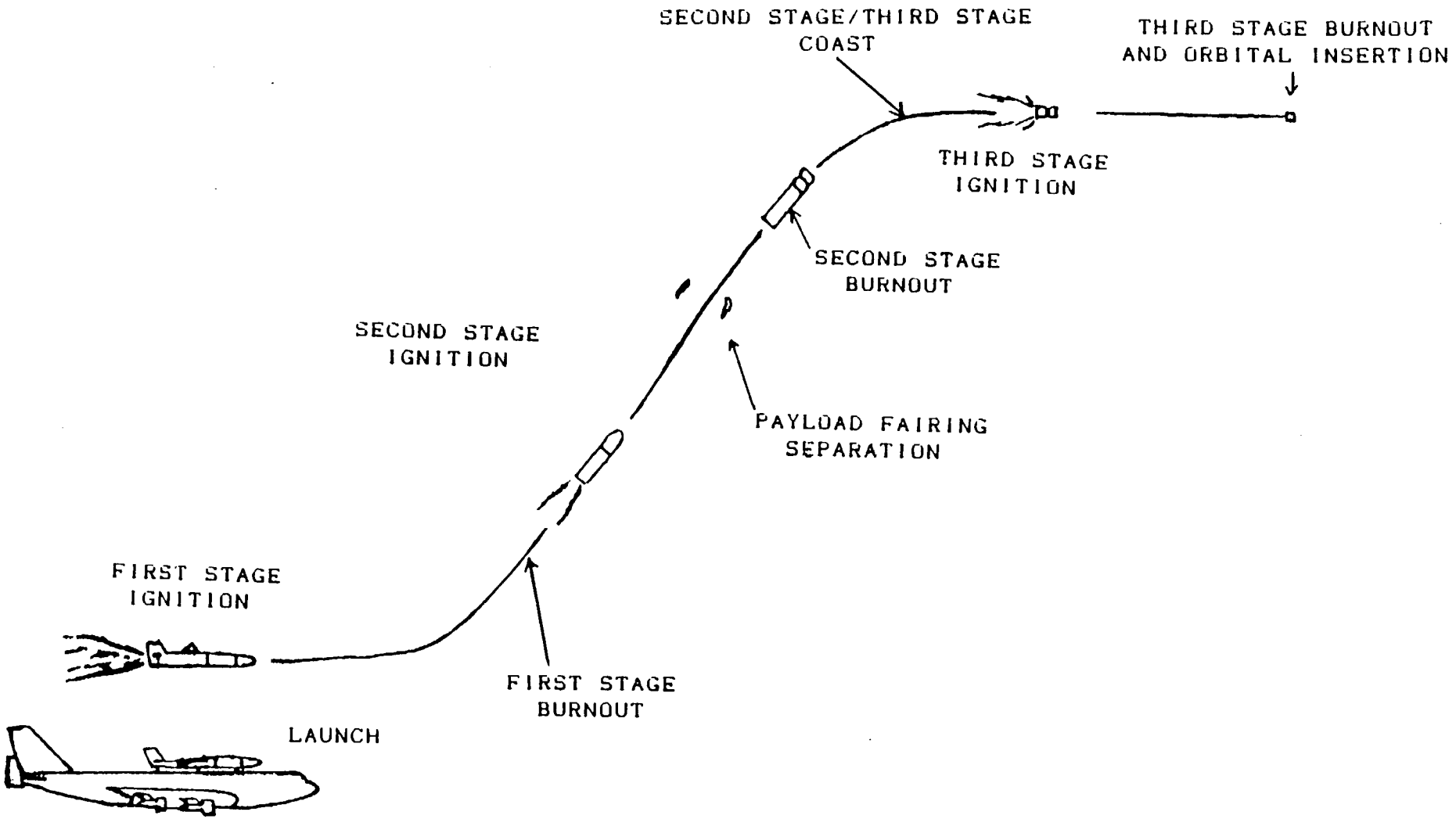

Figure 3: Schematic of LER Trajectory

first stage is dropped. At this point, atmospheric effects become reasonably small due to the absence of the wing. Also, available atmospheric and aerodynamic data are considered to be unreliable.

Several sample missions have been developed for the LER. One of the missions calls for delivering a full 1500 pound payload to the maximum 250 nautical mile orbit. The LER is launched from the 747 over the equator. A brief synopsis of this trajectory is presented. The same series of events occurs during all missions, however the performance numbers change slightly for different trajectories. Mission time begins with first stage ignition.

1. First Stage Burn

The first stage burn begins approximately seven seconds after separation of the LER from the 747. A flight path angle of 10 degrees is maintained until 20 second after first stage ignition. Velocity is about 2,010 feet per second. The flight path angle is raised slowly (no more than 1 degree per second) until a 35 degree angle is reached 56 seconds after ignition. This flight path angle is held until first stage burnout. At burnout, the LER achieves an altitude 122,578 feet above sea level. Velocity is 7,277 feet per second with respect to the launch site. Adding the earth's rotational speed imparted to the LER (variable with launch site), the velocity is 8,623 feet per second.

During the first stage, maximum longitudinal acceleration is 6.4 g's. The maximum lateral acceleration, though, is only 3.8 g's. The lateral accelerations are minimized in order to avoid overstressing the wing surface and fuselage connection. First stage separation is initiated at motor burnout, 61 seconds after ignition. A five second coast period is provided for separation and second stage ignition.

2. Second Stage Burn

The second stage is ignited 66 seconds after first stage ignition and burns for 61 seconds. An emphasis is placed on achieving high longitudinal velocities during this stage; therefore, the flight path angle for the sample mission is reduced to 25 degrees for much of the second stage. The payload fairing is dropped when the LER reaches an altitude of 250,000 feet. For this mission, the fairing drops 104 seconds into the flight. Also, at time equal to 104 seconds into the mission, the sequence to raise the flight path angle to a final burnout value of 38 degrees is started. The LER reaches an altitude of 356,000 feet and a velocity of 15,821 feet per second at second stage burnout. The second stage motor casing drops immediately after burnout.

3. Coast and Third Stage Burn

A rather long coast period is included in the

trajectory after second stage burnout. During this coast period, the LER reaches a very high altitude using momentum in the vertical direction. Optimum time for the coast is calculated with the assumption of zero atmospheric drag and a constant gravitational attraction. For the sample mission, the altitude at the end of coast is approximately 310 nautical miles and the velocity is 14,991 feet per second. The third stage is designed to accelerate the LER to orbital velocities. The third stage raises the velocity of the LER by 10,145 feet per second. Final velocity is 25,136 feet per second. Altitude remains at approximately 300 nautical miles.

Figure 4 shows velocity and altitude profiles versus time for the sample trajectory. The trajectory modeling uses Newton's two dimensional equations of motion for the first and second stages. The coast phase is calculated using the following equations:

$$\text{Time Coast} = \text{Velocity} \cdot \sin(\text{FPA}) / \text{Gravity}$$

$$\text{Altitude Coast} = \text{Velocity}^2 \cdot \sin^2(\text{FPA}) / 2.0 / \text{Gravity}$$

The third stage is modeled assuming a constant specific thrust ratio for the motor:

$$\text{Delta Velocity} = \text{ISP} \cdot \text{Gravity} \cdot \ln \frac{\text{Mass Initial}}{\text{Mass Final}}$$

This model for the LER trajectory proves that the basic

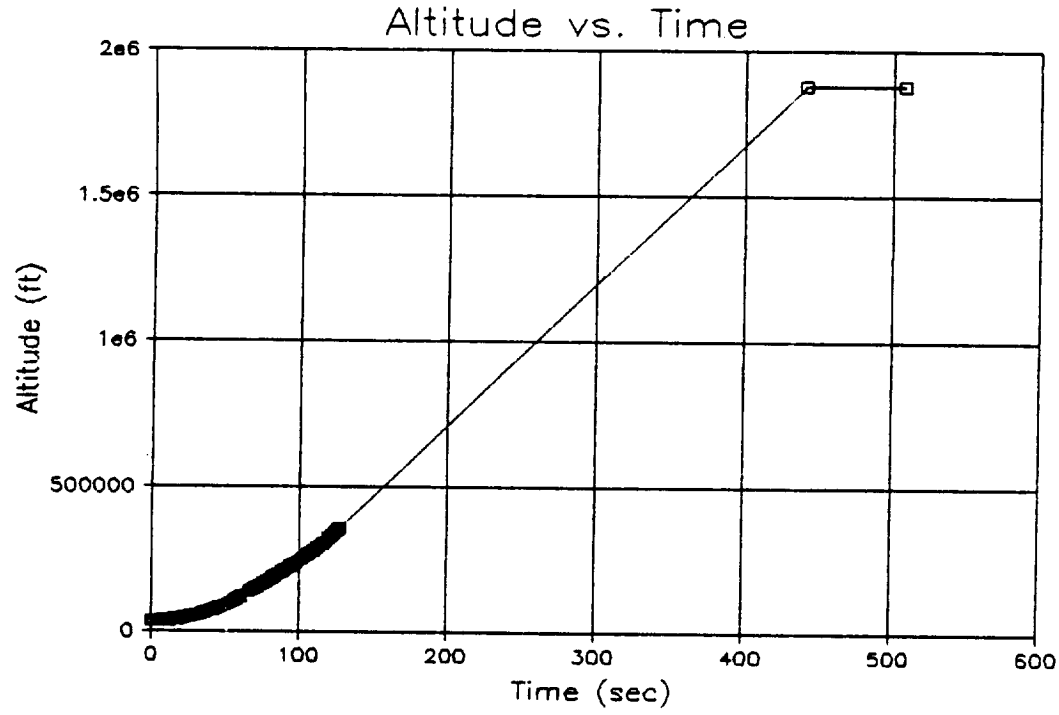

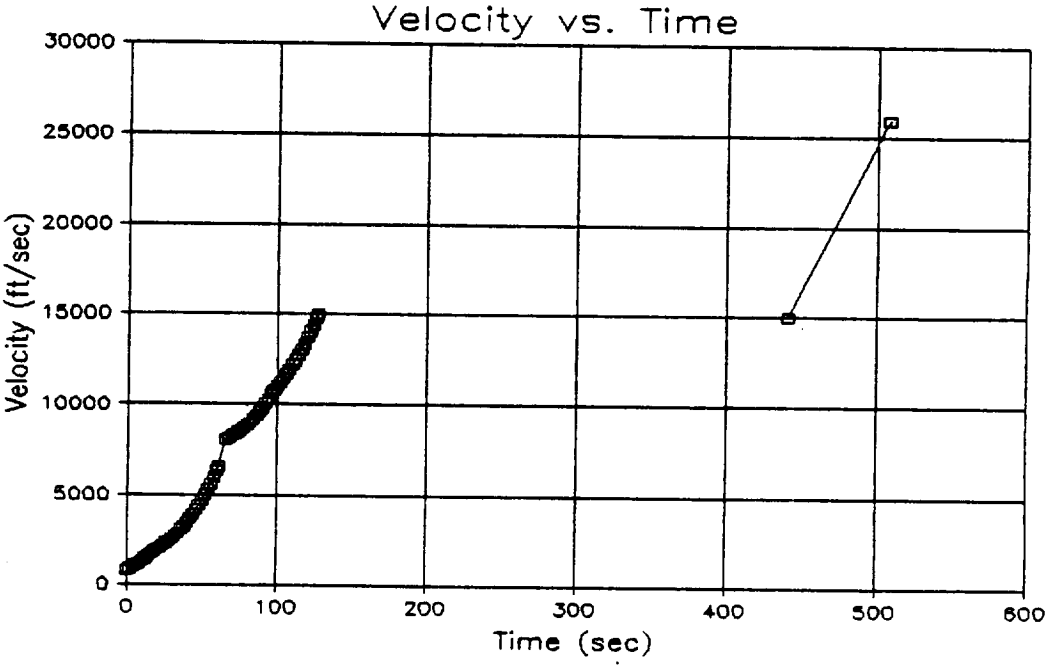

Figure 4: Altitude and Velocity vs. Time for LER Ascent

concept works. Though the altitude of the orbit is higher than desired, many losses are not considered in the trajectory analysis. Another, more accurate trajectory model must be created to perfect and plan specific missions. A copy of the data for this sample mission is included in Volume II.

Aerodynamics

The LER is a cross between a ballistic missile and an airplane. Therefore, the prediction of aerodynamic performance utilizes modern missile and aircraft theories. These two types of analysis are brought together to simulate the actual performance of the LER from launch to first stage burnout. The methodology and assumptions utilized to predict body aerodynamic parameters are presented first, followed by the wing and tail methodology.

In flight, the LER body will experience two primary types of drag forces. The first type of drag force is skin friction drag and is caused by air viscosity. The second type of drag force is pressure drag and is due to differences in pressure on the surface. Since the LER body is assumed to be non-lifting, induced drag is not present.

Skin friction drag is dependent upon the type of flow (laminar or turbulent) and the Reynold's number. For laminar incompressible flow, the skin friction coefficient is given by the Blasius solution:

$$Cfl = 1.328/(RN)^{.5}.$$

For turbulent incompressible flow, the Schoenherr solution is used to determine the skin friction coefficient:

$$(Cft)^{.5} \log(Cft)\ RN = 0.242.$$

Figure 5 shows the skin friction coefficient versus Reynold's number for incompressible flow. This graph indicates that at higher Reynold's numbers, the skin friction coefficient does not change appreciably. The Reynold's number for the first stage LER trajectory varies from 1.318 x 10^8 to 1.13 x 10^9. Consequently, the laminar skin friction coefficient is assumed to be a constant 1.1 x 10^-4 and the turbulent skin friction coefficient was assumed to be a constant 16 x 10^-4.

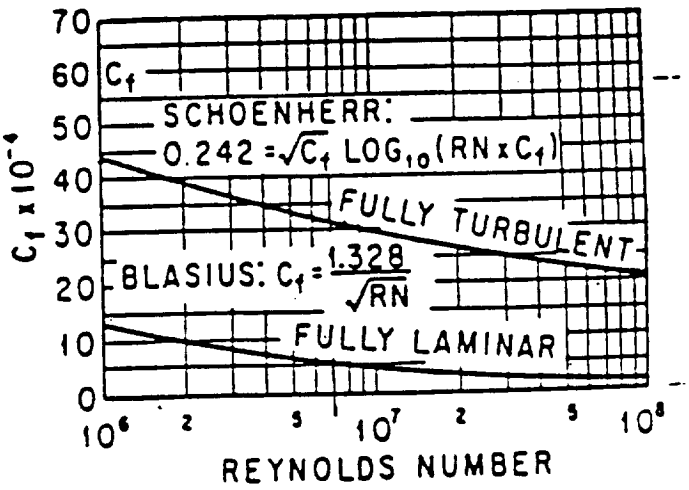

Figure 5. Skin friction coefficient versus Reynold's number for incompressible flow (Chin:65).

The LER will experience subsonic flight for only the first few seconds of the mission. For the remainder of the flight, transonic and supersonic speeds are encountered. Therefore, the Mach number effects must be considered. For laminar flow, the following expression can be used to determine the effect of compressibility:

$$\frac{C_{f_\ell}}{C_{f_c}} = \left(\frac{1}{1 + 0.85M^2/5}\right)^{0.1295}$$

where M is the Mach number. For turbulent compressible flow, the extended Frankl-Voishel theory is used:

$$\frac{C_{f_t}}{C_{f_c}} = \frac{1}{\left(1 + \frac{\gamma-1}{2}M^2\right)^{.467}}$$

The methodology used in incompressible flow for determining the transition point is also used for compressible flow.

The coefficient of drag due to skin friction is determined using the following relation:

$$CD = Cf * Swetted/Sref$$

For proof of concept design purposes, the skin friction drag coefficient should be increased by 10% to account for surface roughness.

Pressure drag has two possible components: pressure drag about the nose and base pressure drag. Base pressure drag is caused by the flat area at the base of the missile fuselage. This type of drag is approximately zero during subsonic

flight, and can be approximately zero during supersonic flight when the motor is running. Since the rear nozzle's exit diameter is equal to the fuselage diameter, base pressure drag for the LER is approximately zero.

The nose design used on the LER is a tangent ogive. This type of nose offers good strength, drag, and payload area characteristics. The pressure drag estimation method used for the LER was developed by E. R. C. Miles from experimental data. The coefficient of drag is estimated as:

$$C_{D_f} = P\left\{1 - \frac{2[196(\ell/d)^2 - 16]}{28[M+18][\ell/d]^2}\right\}$$

where P is given by

$$P = \frac{\Delta P}{q} = \left(0.083 + \frac{0.096}{M^2}\right)\left(\frac{\sigma}{10}\right)^{1.69}.$$

The ogive semi-vertex angle at the tip of the nose is given by:

$$\sigma = 2\tan^{-1}\left(\frac{1}{2\ell/d}\right)$$

Therefore, with the coefficients of drag available for each the skin friction and pressure contributions, the total drag of the body can be estimated by:

$$CD = CD\ (\text{skin friction}) + CD\ (\text{pressure}).$$

Table 4 lists the coefficients of drag of the body based on body frontal area for the Mach number range of the first stage part of the mission.

Table 4: Coefficient of Drag for the Body

Mach Number	Friction Drag Coefficient	Pressure Drag Coefficient	Total Drag Coefficient
0.8	0.0767	1.2388	1.3155
1.0	0.0714	0.9734	1.0448
2.0	0.0591	0.6427	0.7018
3.0	0.0481	0.6109	0.6590
4.0	0.0398	0.6221	0.6619
5.0	0.0337	0.6441	0.6778
6.0	0.0291	0.6690	0.6981
7.0	0.0256	0.6941	0.7197
8.0	0.0239	0.7185	0.7424

Much of the wing analysis is conducted using the theories and prediction methods in the British Data Sheets, published by the Royal Aeronautical Society in 1957. Although not perfect, the British Data Sheets are a good source of preliminary information for proof of concept purposes.

Several assumptions are used during the analysis of wing performance. The major assumptions used are flat wing theory and elliptical loading. These assumptions are justified since the wing has a low thickness to length ratio and wings of similar planforms exhibit elliptical loading characteristics. Other assumptions used include a fully turbulent boundary layer over the entire wing and zero heat

transfer. Mission profile considerations and the nonreusalibility of the structure deem such assumptions valid.

The drag of the wing surface consists of several parts:

$$CD = CD(skin) + CDo + CD(wave) + CD(angle\ of\ attack)$$

Skin friction drag is approximated using British Data Sheet S.02.04.12. British Data Sheet S.02.04.01 is utilized to determine zero lift drag. In each case, the upper velocity of the LER is above the data available from the data sheets. It is necessary to extrapolate to either the appropriate Mach or Reynolds number required. Extrapolation is acceptable for two reasons; the data is fairly linear and aerodynamic effects are small at the high Mach numbers for the LER due to the high altitude.

Table 5 lists the approximate total zero incidence drag term for the wing over the Mach range. The values listed are computed using the drag equation above, with an added twenty percent attributed to wing thickness and surface roughness.

Wave drag becomes an important term as the Mach number of the wing rises above 1.0. This drag is due to the shock wave which forms on the leading edge of the wing. Wave drag can be modeled for a flat plate wing using:

$$C_{D_w} = \frac{4\alpha^2}{(M^2 - 1)^{1/2}}$$

Table 5: Zero Incidence Coefficient of Drag of the Wing

Mach Number	Skin Friction Coefficient	Plate Drag Coefficient	Total Drag Coefficient
0.8	0.0055	0.0055	0.0140
1.0	0.0050	0.0050	0.0120
2.0	0.0030	0.0045	0.0090
3.0	0.0025	0.0040	0.0078
4.0	0.0020	0.0040	0.0072
5-8	0.0018	0.0040	0.0070

It should be noticed that the value of wave drag changes with the angle of attack. Flat plate theory assumes that wave drag due to wing thickness is zero.

Much of the drag on the wing, especially at separation, is due to incidence drag. Using elliptical loading theory, incidence drag can be stated as:

$$C_{D_i} = \frac{C_L^2}{\pi \cdot AR \cdot e}$$

where e is Oswald's efficiency factor. This factor is expressed as:

$$e = \frac{1}{(\pi \cdot AR \cdot K) + 1/uS}$$

where k, u, and s are empirical quantities. Oswald's efficiency factor for the LER is estimated as 0.88.

Wing lift approximations also utilize the British Data

Sheets. Sheet number S.01.03.05, which predicts wing lift for a flat wing of approximately the shape of the LER wing, is used for lift calculations. The lift equation used is:

$$CL = CLo + CL(\text{angle of attack}).$$

Using flat plate theory, the zero incidence lift term, CLo, is assumed to be approximately zero. Table 6 lists the approximate coefficient of lift per angle of attack as determined from the data sheets.

Table 6: Coefficient of Lift per Radian Angle of Attack for the Wing

Mach Number	CL/(angle of attack)
0.75	7.05
1.00	7.85
1.25	5.25
1.50	3.55
1.75	2.75
2.00	2.00
3.00	1.00
4.00	0.50
5.00	0.38
6.00	0.33
7.00	0.28
8.00	0.23

As can be seen, the lift coefficient drops as the Mach number increases, as expected. The data beyond Mach 2.0 is extrapolated.

The tail analysis is greatly simplified by assuming a non-lifting tail. This assumption is considered valid for early proof of concept analysis. The coefficient of drag of each tail surface is equivalent to the wing using flat plate theory (see Table 5). However, in magnitude, the drag of the tail surfaces is much less due to the smaller area.

The total drag for the LER is determined by adding the body drag, the wing drag, and the tail drag for each tail surface. Once this value has been determined, an extra 10% is added to include interference factors.

Therefore, knowing the coefficients of lift and drag for the LER at each Mach number, an approximation of lift and drag over the first stage flight can be made. Lift and drag for the LER during first stage flight are calculated by the mission trajectory software.

Figure 7 is a plot of lift and drag versus altitude during first stage burn for the sample trajectory. As can be seen, the lift over drag ratio is very high, over 9 to 1 at one point. The wing lift is predicted to be of enough aid to the ascent to outweigh the drag losses.

The major purpose of the wing, however, is to lift the LER from the back of the 747 during separation. Without a large wing, a system would be required to push the LER off the back of the 747, clearing the vertical tail. Such a

system, though possible, would be heavy and expensive. Therefore, wing lifting of the LER during separation is a design requirement. The present wing is sized for separation lift, not for trajectory optimization.

At separation, the flight conditions and the weight of the LER is known. The wing, neglecting 747 interference, provides 68,000 pounds of lift at a Mach number of 0.8, altitude of 35,000 feet, and an effective angle of attack of 10 degrees. This lift provides 1.11 g's of upward acceleration at separation. Boeing 747 interference effects are actually expected to aid separation. Upwash from the nose raises the effective angle of attack of the LER. Full wind tunnel testing is necessary to determine all interference effects.

Vortex imaging of the LER wing and tail surfaces, along with wind tunnel testing, will be accomplished before full scale developmental modeling is attempted. Wind tunnel testing of the LER mated to the 747 is necessary to validate and optimize ferry and separation techniques.

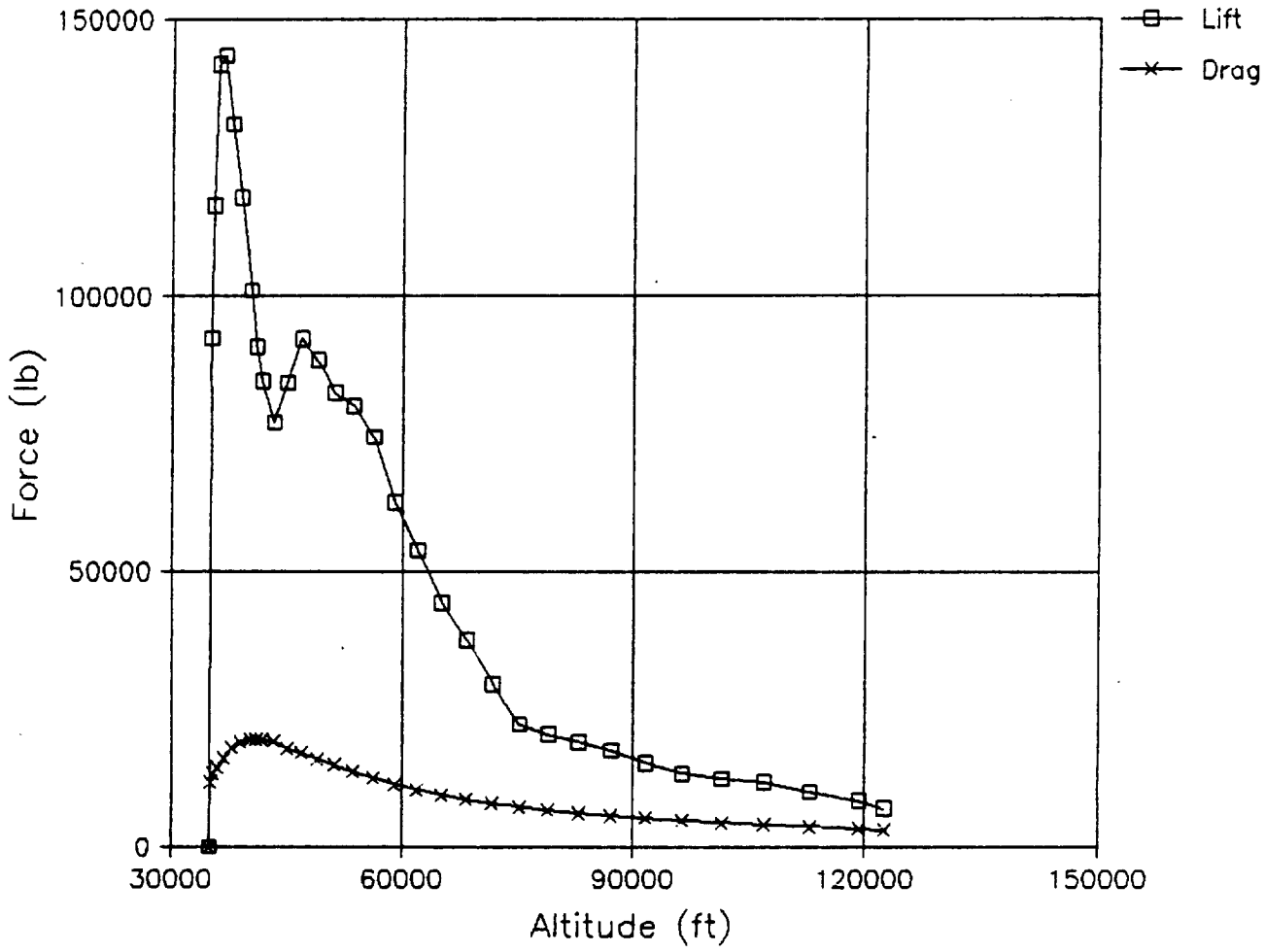

Figure 7: Lift and Drag vs. Altitude for LER Ascent

Propulsion

The propulsion design consists of two separate parts. The grain configuration and propellant types are chosen with certain performance goals. The nozzles and thrust vectoring systems are designed to maximize motor thrust. An overview of each section is presented.

1. Grain Configuration

Once the mass flow rate has been determined for the desired thrust, the grain configuration must be designed to produce that mass flow rate over the required burn time. The first item to be calculated is the area of burn for mass flow. This calculation is accomplished by using the following relation:

$$A_b = \dot{m} / r \rho$$

where the r is the burn rate of the propellant, ρ is the propellant density and m is the mass flow rate.

After the burn area has been determined, the next critical choice is grain design. For the LER, it is desired to have a constant mass flow rate at all times, achievable by keeping the area of burn as constant as possible.

The star shape grain design was chosen because it is believed to have a more constant burn area than a cylindrical grain. For the LER, a three point star is chosen (see Figure 8). The process of calculating the burn circumference of the

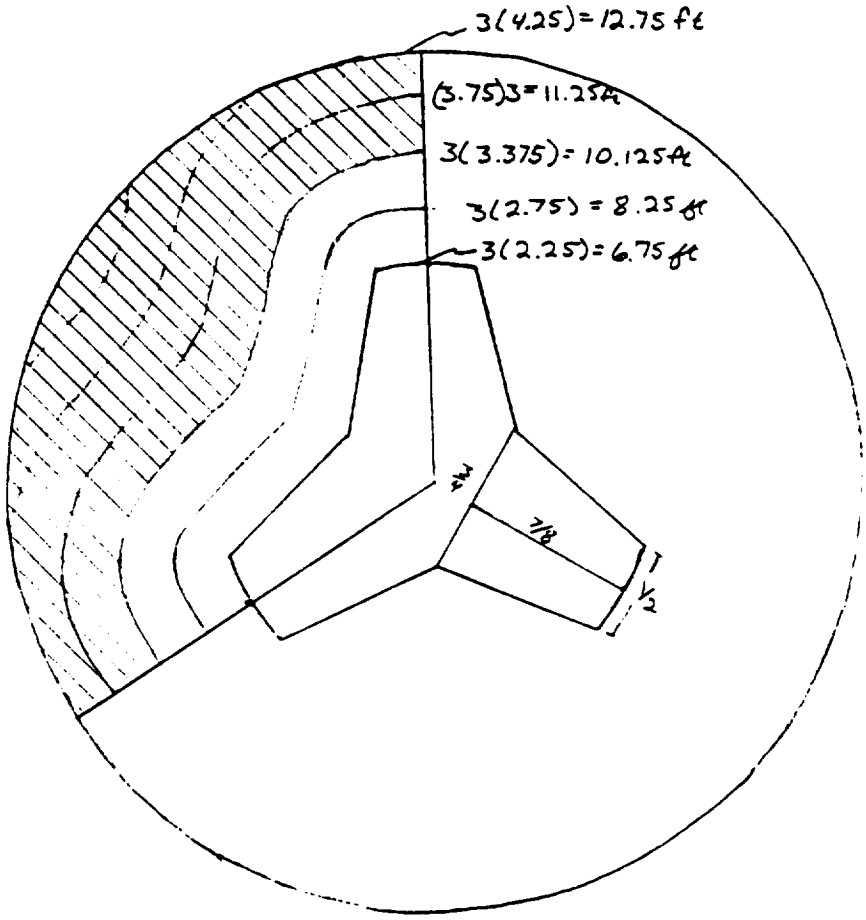

Figure 8: Cross Sectional View of 3-Point Grain Design

cross section of the rocket stage is simple. The length of the grain can be determined from the circumference. It is of chief importance to keep the grain size of the propellant within the size limitations set by the aerodynamic and structural designs.

To calculate the burn time the mass of the propellant must to be determined. The volume of the propellant can be obtained by subtracting the volume of the shape of the grain. With the resulting volume, the mass can determined by multiplying the density of the propellant and the volume. The time to burn out can now be calculated by dividing the mass flow rate into the total mass. However, this time to burn out is only good for a constant burn rate and area, which has not yet been determined.

To determine if the mass flow rate is constant, a scaled cross section is drawn of the grain configuration. By tracing the grain design with a compass the regression of the propellant is determined as well as the mass flow.

With this trace, measurements can be made of the circumference of each trace as well as the distance from the original grain configuration. By plotting circumference versus regression, the burn area can be calculated by multiplying the circumference by the length of the grain (see Figure 9)

At this point, a relatively accurate picture of the mass flow and combustion pressure can be predicted. By assuming that at time equal zero seconds the motor is running at the

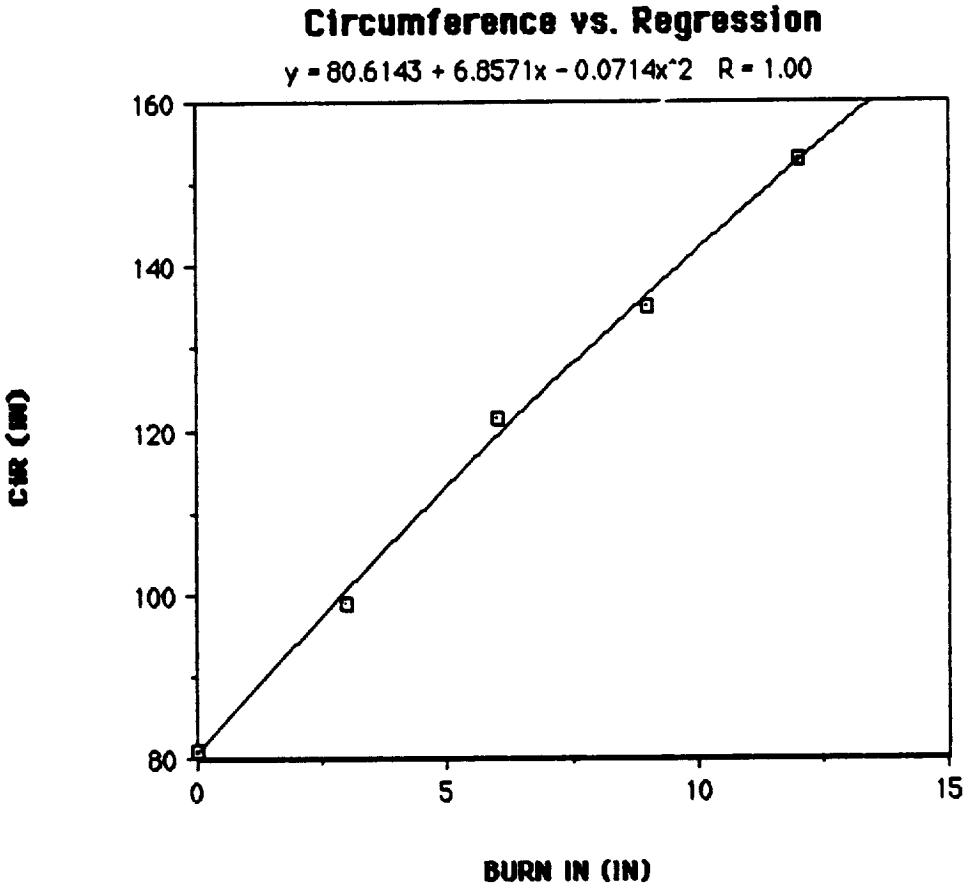

Figure 9: Circumference vs Regression for LER Motors

initial condition of a known combustion pressure, the burn rate can be determined by the equation:

$$r = aP_c^n$$

where a is the coefficient of the propellant, n is the combustion index, P_c is the combustion pressure, and r is the burn rate of the propellant.

By setting a delta time interval (1 second, for example) the regression of the grain can be determined by multiplying this time unit by the burn rate. This method assumes that over the delta time the burn rate is constant; therefore the smaller the time unit the better the results.

The area of burn is determined on the plot of circumference versus regression of the propellant; and this burn area is used to calculate the mass flow rate at time t:

$$m = A_b r \rho.$$

The combustion pressure is determined by:

$$P_c = c^* \dot{m} / A_* g_c$$

where A_* is the throat area, c^* is the characteristic velocity, g_c is the gravitational constant, $\dot{m}$ is the mass flow rate, and P_c is the combustion pressure at time t.

This process is repeated for each time interval until

the mass spent is equal to the original mass of the propellant.

This process revealed that the combustion pressure and burn rate rise sharply with a small increase in burn area. Structurally, low combustion pressures are a necessity. Therefore, a propellant change is required to ensure low burn pressures. A second, slower burning propellant is located on the outer circumference of the faster burning inner propellant. When the combustion pressure reaches maximum allowable limits, the second grain is designed to ignite. The substitute of the second grain causes a rapid drop in the pressure and the mass flow. A decrease in thrust occurs, but the thrust soon returns to prior levels.

The propellants chosen for the LER project are hydroxl-terminated polybutadiene (HTPB) and polyurethane (PU). HTPB burns quickly, making it a good choice at motor ignition when high thrust is a necessity. PU, the slower burning propellant, allows a long burn without high combustion pressures.

Even though this grain design works, it can most certainly be improved by the contractors of the motor. This design proves, however, that solid rocket motors can be designed to perform to the specifications required by the LER system.

2. Nozzle Analysis and Design

The characteristics of the nozzles used in each of the three stages are given in Tables 7, 8, and 9. The nozzle for stage one is a fixed nozzle arrangement whereas the nozzles for stages two and three are movable nozzles directing thrust for rotation about the y and z body axes. Several assumptions were used in the analysis regarding exhaust gas flow and composition.

1. The composition of the product gases entering a nozzle varies greatly depending upon given combustion conditions. Once in the nozzle, exhaust gases can change composition erratically with prediction of such behavior difficult at best. With this variance, a variation occurs with the gas constant, R, of the exhaust gases as well as the specific heats, Cp, and the ratio of specific heats, γ. These variables are used extensively in nozzle analysis and can usually be obtained from the propellant supplier via Strand Burner test data. Since this data is not readily available, the following values were assumed upon the advice of an instructor:

Ave. Molecular Wt of Exhaust Gases	30.0 lbm/lbm mole
Ratio of Specific Heats (γ)	1.2

These assumptions led to some error during the analysis because ordinarily these two variables are directly related. These errors could be eliminated with more detailed propellant data.

2. The analysis assumes steady, gaseous flow in a chemical equilibrium which does not change within the nozzle for small time increments. Transient conditions are not considered.

3. The method used in the preliminary nozzle analysis assumes frictionless, adiabatic flow. This assumption is used frequently in preliminary design work and usually predicts actual nozzle performance within 1-8%. The use of smooth nozzle surfaces and insulative materials aids in substantiating this assumption. For this analysis, the thrust values obtained from these ideal assumptions were decreased by 4% to yield the expected real thrust values shown in Tables 7, 8, and 9.

Chamber pressure in the first stage was desired to be kept as low as possible to allow for minimum structural weight. To eliminate flare drag from the nozzle, it was desired to keep the nozzle exit area no larger than the cross sectional area of the booster itself. These requirements, along with a desired first stage average thrust of at least

125,000 lbs., dictated the design of the first stage nozzle. The first stage booster is to fly at altitudes ranging from 35,000 ft. to 210,000 ft. Various ratios of chamber pressure to exit pressure were obtained from these altitudes and used to determine a "first guess" average ideal specific impulse of 275 seconds according to the equation

$$Isp = \sqrt{\frac{2R}{g_c}\left(\frac{\gamma}{\gamma-1}\right)\frac{T_c}{M}\left(1-\left[\frac{P_e}{P_c}\right]^{\frac{\gamma-1}{\gamma}}\right)} + \frac{(P_e-P_a)A_e}{\dot{m}}$$

With minimal average thrust and specific impulse determined for the initial design analysis, the mass flow rate of exhaust gases through the nozzle was calculated to be about 477 lbm./sec. Combustion pressure was initially set at 500.0 psia.(total pressure) and was assumed constant from the combustion chamber to the nozzle inlet. Using the mass flow rate equation in terms of total conditions,

$$m = P_c A^* \sqrt{\frac{\gamma g_c}{R/M\ T_c}\left(\frac{2}{\gamma+1}\right)^{\frac{\gamma+1}{2(\gamma-1)}}}$$

a corresponding throat area can be calculated. A low value for the ratio of exit area to throat area is desired to keep the nozzle as short as possible, and the exit area is to be no larger than the booster cross sectional area. With these variables defined, the nozzle exit area, and thus a design altitude, can be calculated first by solving the equation

$$Ae/A^* = \frac{1}{M_e}\left[\frac{1 + \frac{\gamma-1}{2} M_e^2}{\frac{\gamma+1}{2}}\right]^{\frac{\gamma+1}{2(\gamma-1)}}$$

for nozzle exit Mach number, and then finding the corresponding exit pressure using the relation

$$Pc/Pe = \left(1 + \frac{\gamma-1}{2} M_e^2\right)^{\frac{\gamma}{\gamma-1}}$$

The performance of the motor at various altitudes for a constant mass flow stage can then be easily evaluated.

After considerable trajectory analysis, it was determined that the constant mass flow stages originally considered were inadequate, and thus each of the three stages were redesigned to provide a progressive burn. Performance analysis for the progressive burn stages was carried out using the same equations as for the constant burn stages. The analysis, however, was done for many small time steps to include the effects of increasing mass flow rate, chamber pressure, and exit pressure as well as decreasing atmospheric pressure with increasing altitude. The results of the stepwise performance analysis for each stage is shown graphically in Figures 10,11, and 12.

The length of a conical nozzle can be determined from a given ratio Ae/A* by assuming a nozzle cone divergence half

angle and using the law of sines. This equation in final form is

$$l = \frac{\frac{1}{2}(d_e - d_*)\sin(90-\alpha)}{\sin\alpha}$$

The length, l, is the length of the diverging portion of the nozzle. Length of the converging portion of a nozzle was chosen to be 15% of the length of the diverging portion. Conical nozzles are simple, easy to manufacture and can be optimized for divergence half angles of between 12 and 18 degrees. Bell-shaped, or contour nozzles frequently used in liquid rockets are shorter, and thus lighter than conical nozzles. Contour nozzles, however, experience higher losses in solid propellant gas flow and are therefore not advantageous over the simpler conical design. The nozzles used on each stage of the LER use conical nozzles of 18 degree divergence half angles.

The material chosen for the nozzles was Udimet 500, a high quality, high strength steel particularly useful at extreme temperatures. The throat and portions of the converging section of the nozzles are lined with molded graphite to protect against throat erosion and excessive heat transfer. The diverging portion of the nozzles are protected from extreme temperatures by a coating of ablative plastic (Figure 13).

Thrust vectoring on the second and third stage motors is achieved with movable nozzles (Figure 13). The basic design

chosen for the LER is a flexible bearing design. With the use of two actuators, each nozzle is capable of a vectoring angle of approximately 10 degrees. Advantages of the flexible bearing design include reliable sealing around the joint and the elimination of sliding parts exposed to hot gases.

Table 7. Nozzle Design Characteristics - First Stage

Nozzle Type	Fixed
Divergence Cone Half Angle	18 degrees
Design Altitude (approx.)	41,000 ft.
Expansion Area Ratio (Ae/A*)	19.19887
Total Nozzle Length	6.829 ft.
Exit Area	2,827.44 in.^2
Throat Area	147.271 in.^2
Maximum Upstream Pressure	807.54 psia.
Maximum Exit Pressure	4.319 psia.
Maximum Mass Flow Rate	771.203 lbm./sec.
Average First Stage Thrust	153,721 lbf.

Table 8. Nozzle Design Characteristics - Second Stage

Nozzle Type	Movable
Divergence Cone Half Angle	18 degrees
Expansion Area Ratio (Ae/A*)	29.544
Total Nozzle Length	6.017 ft.
Exit Area	1963.4 in.^2
Throat Area	66.46 in.^2
Maximum Upstream Pressure	689.8 psia
Maximum Exit Pressure	2.233 psia
Maximum Mass Flow Rate	297.326 lbm./sec.
Average Second Stage Thrust	59,051 lbf.

Table 9. Nozzle Design Characteristics - Third Stage

Nozzle Type	Movable
Divergence Cone Half Angle	18 degrees
Expansion Area Ratio (Ae/A*)	22.14172
Total Nozzle Length	3.164 ft.
Exit Area	706.85 in.^2
Throat Area	31.924 in.^2
Maximum Upstream Pressure	503.0 psia.
Maximum Exit Pressure	2.191 psia.
Maximum Mass Flow Rate	104.136 lbm./sec.
Average Third Stage Thrust	21,744 lbf./sec.

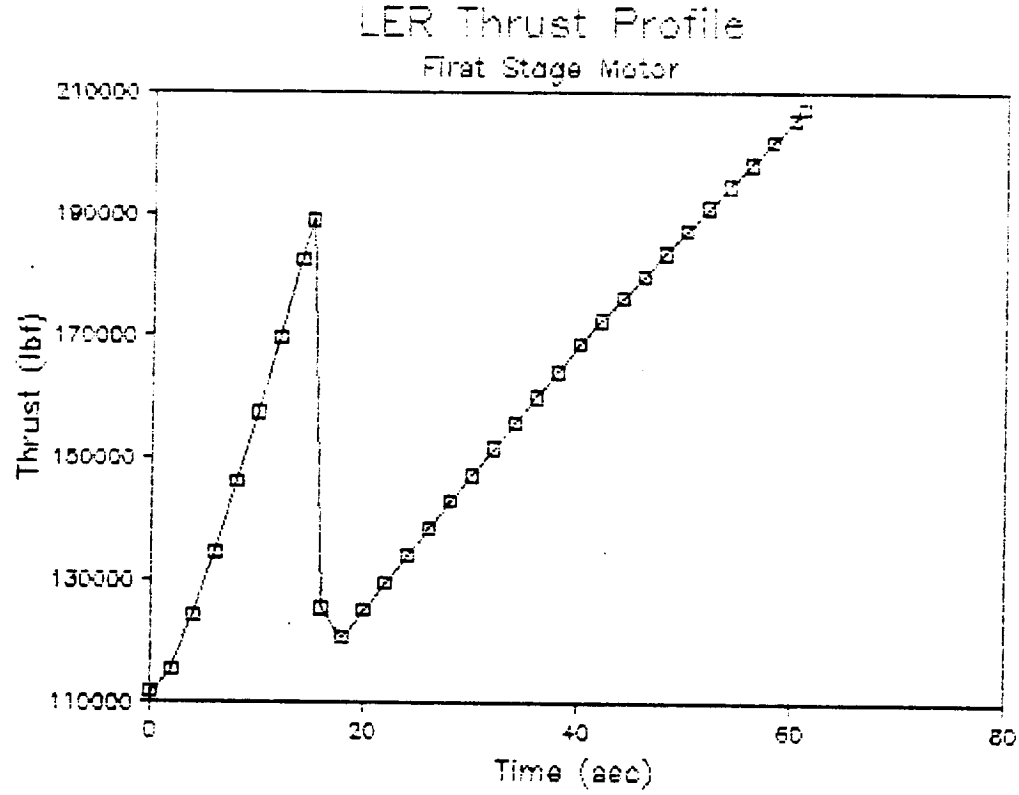

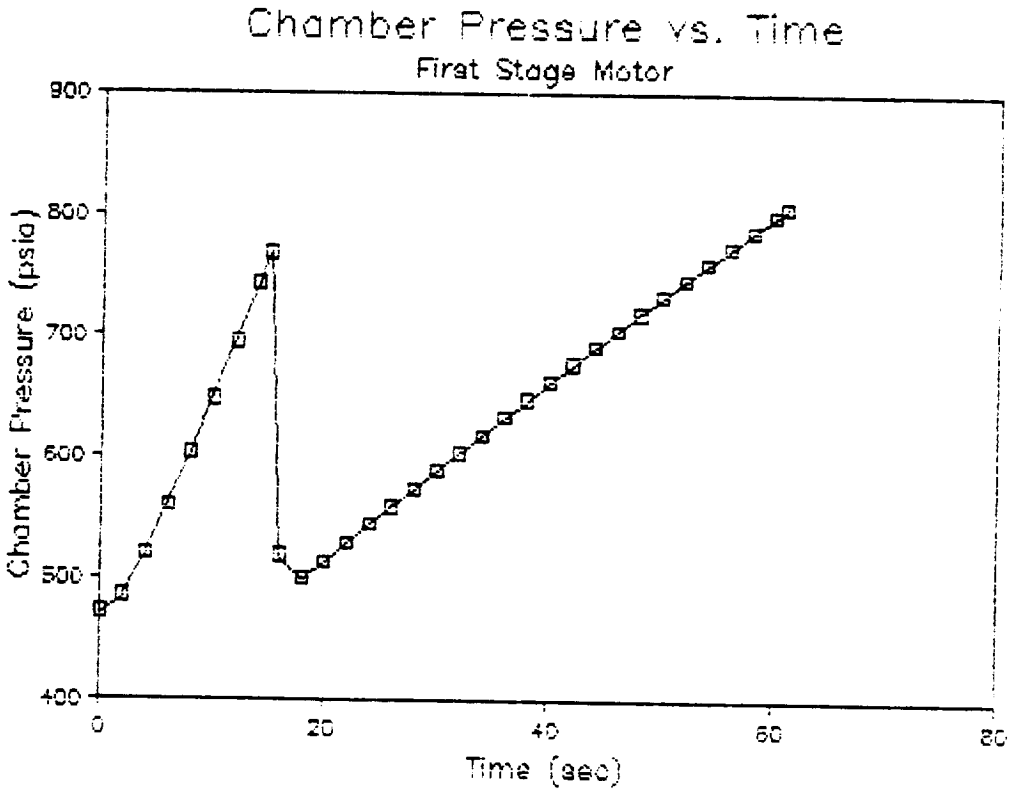

Figure 10: Thrust and Pressure vs Time for First Stage Motor

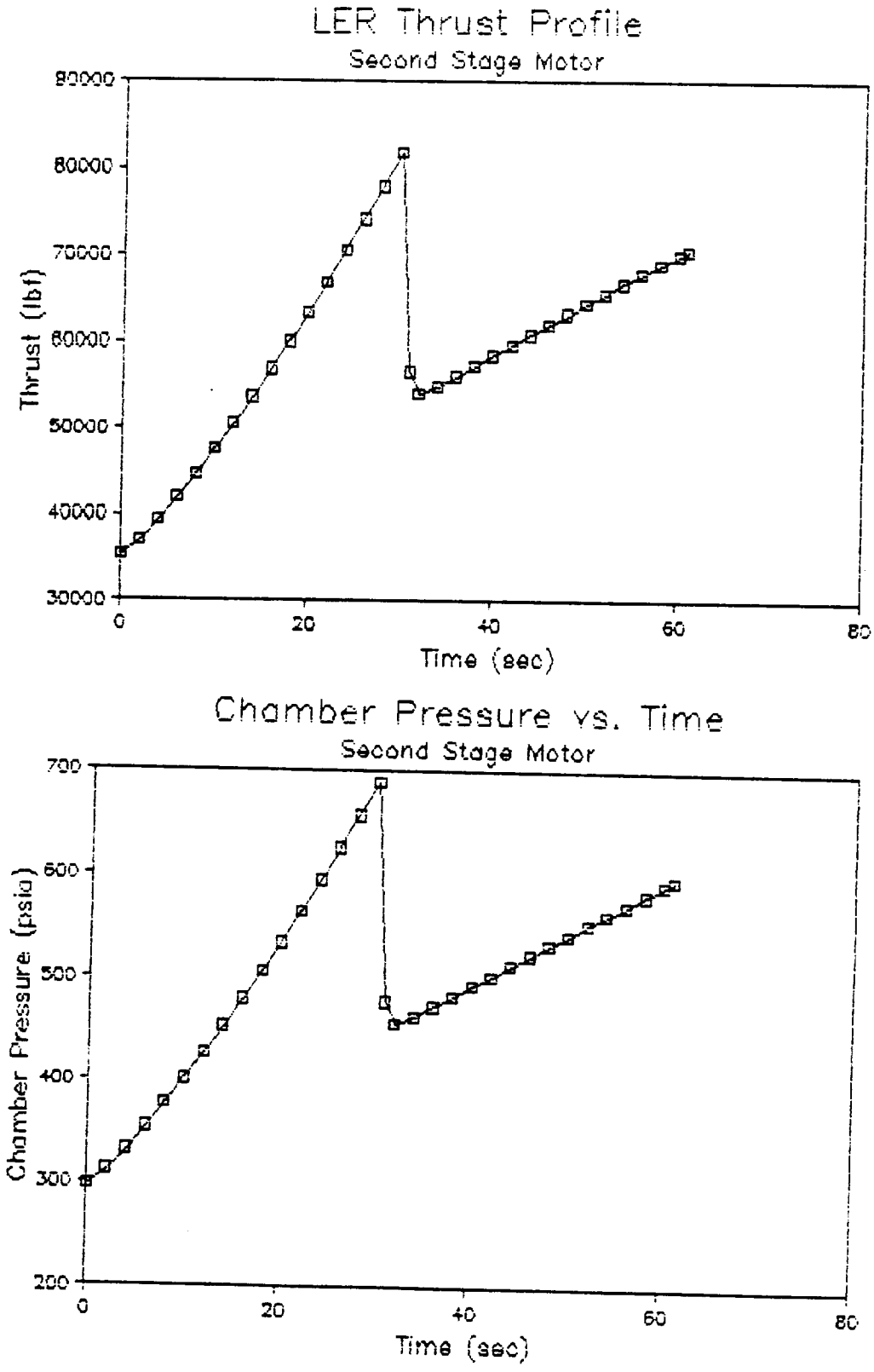

Figure 11: Thrust and Pressure vs Time for Second Stage Motor

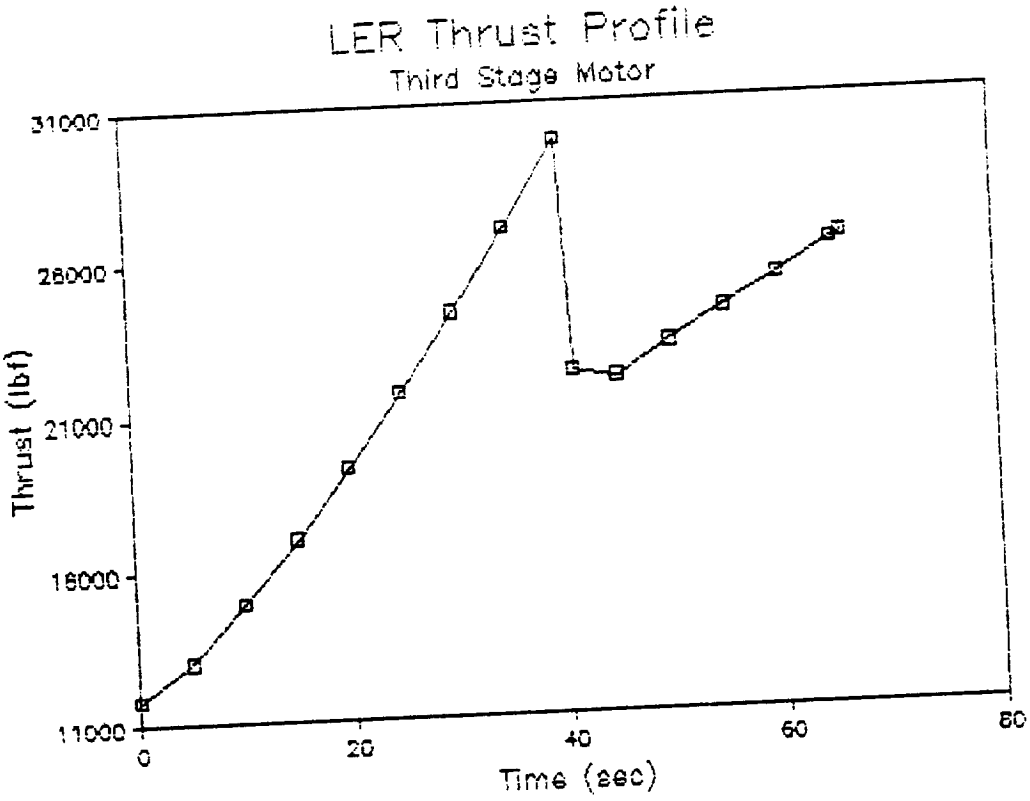

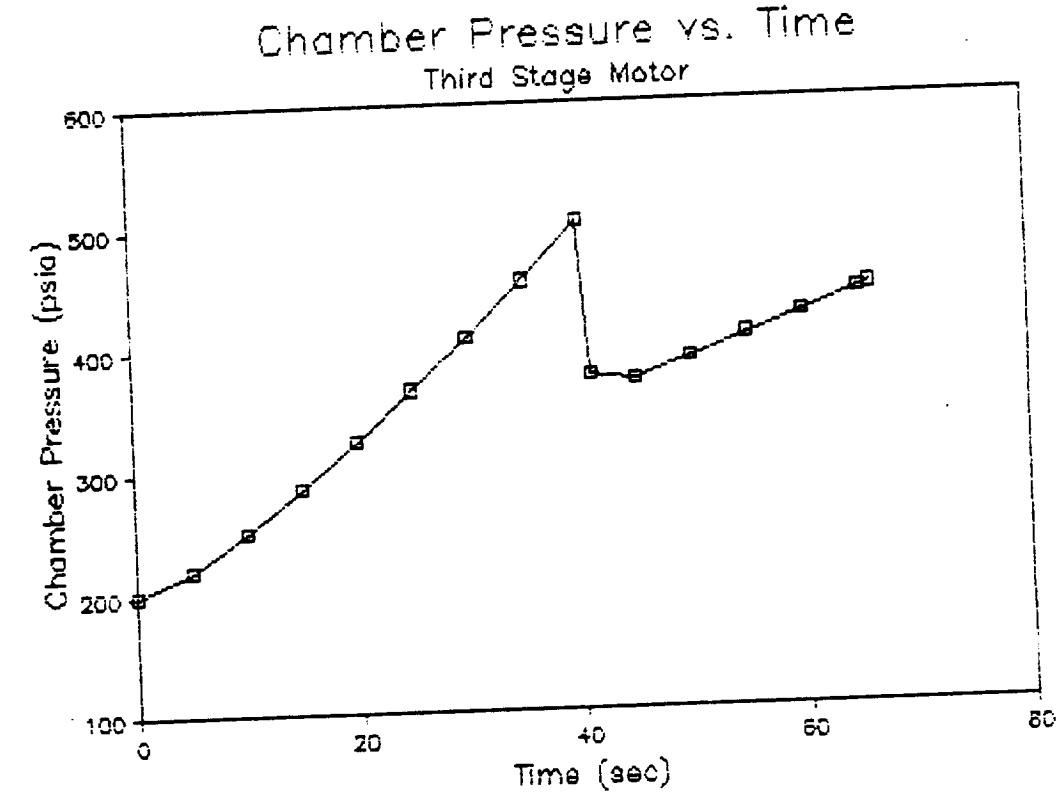

Figure 12: Thrust and Pressure vs Time for Third Stage Motor

Movable Nozzle Design - Second and Third Stages

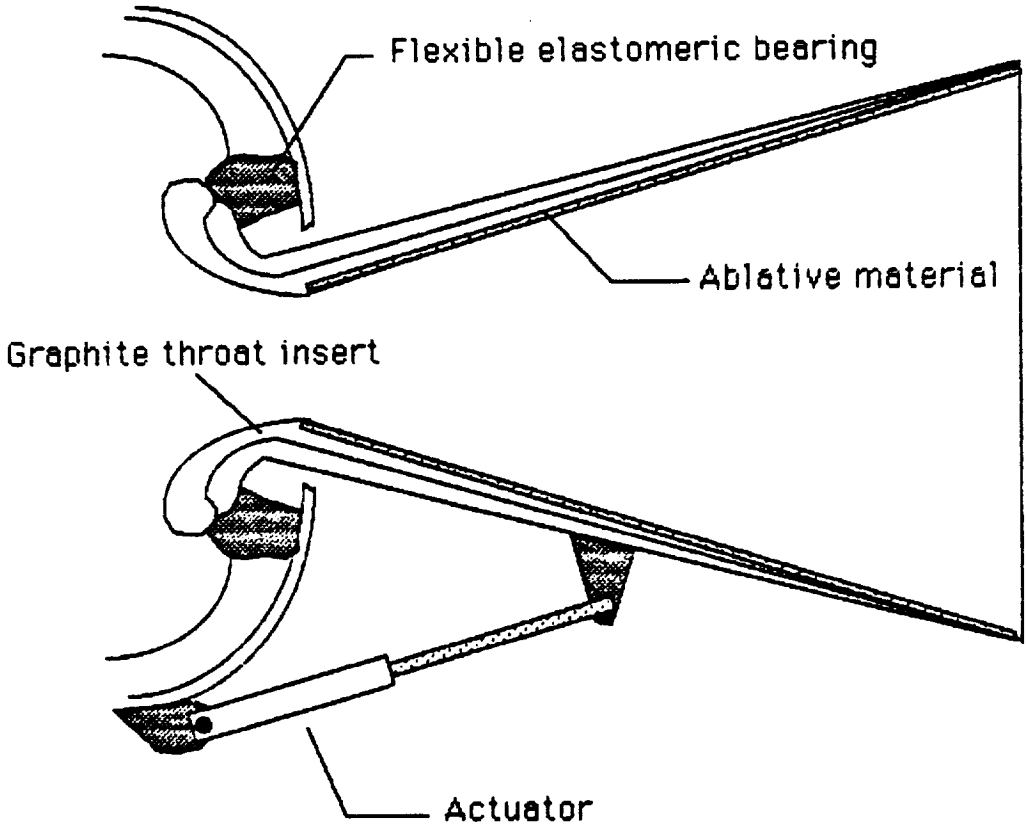

Figure 13: Movable Nozzle Design for Second and Third Stage Motors

Materials

Ballistic vehicle structures require strict design requirements. Materials are required to be very strong while being very light. Selecting such a material to satisfy both requirements is difficult. The structure must be designed to contain the propellant, support engine loads, withstand ground handling and transportation, pre-launch conditions, flight conditions, staging, thrust vectoring, and support the payload with the least possible weight of materials. The structure by design is required to be pushed to its loading limits.

Materials with high specific stiffness and strength must be used. Materials considered for the LER's solid rocket motor casings were Aluminum alloys, Magnesium alloys, and a graphite epoxy composite. See Table 10 for a list of material properties. Aluminum 7178-T6 is a ultra-high strength alloy and a composite matrix of Thornel-400 and epoxy were found to be the best possible booster casing materials. Magnesium alloys were eliminated due to the relative high cost and the prohibitive volume of the material to carry and support loads. Figure 14 shows the costs of common engineering materials. The aluminum 7178-T6 alloy and the Thornel-400 meet the requirement of high strength and low weight. The composite has a large weight advantage over the aluminum 7178-T6 of almost a eleven hundred pounds for the first stage, which gives it a large advantage over the aluminum alloy, since first stage weights are critical.

Table 10: Properties of Materials Under Consideration for Structural Applications

	Ftu (ksi)	Fty (ksi)	Fcy (ksi)	Fsy (ksi)	Density (lb/in^3)
Al 7178-T6	78	68	69	39	0.102
MgA231B-H24	39	29	29	17	0.065
Thor400-Epxy (45 deg weave)	128	102	52	48	0.057

Recent advances in composite fabrication techniques have made composites price competitive with metal alloys.

Effects of temperature and moisture effects were also considered in selection. Both materials lose strength with elevation in temperature. It is apparent that it will be necessary to thermally shield the solid rocket motor casing with a graphite-Asbestos insulation. Aluminum is not appreciably affected by moisture. Aluminum also tends to produce a very hard oxidation layer, which prevents further oxidation. This oxidation makes aluminum attractive if a long period of storage is considered. Thornel-400 epoxy gains very little water content if stored properly in low humidity conditions. The material degradation can be held within reasonable bounds for short storage periods.

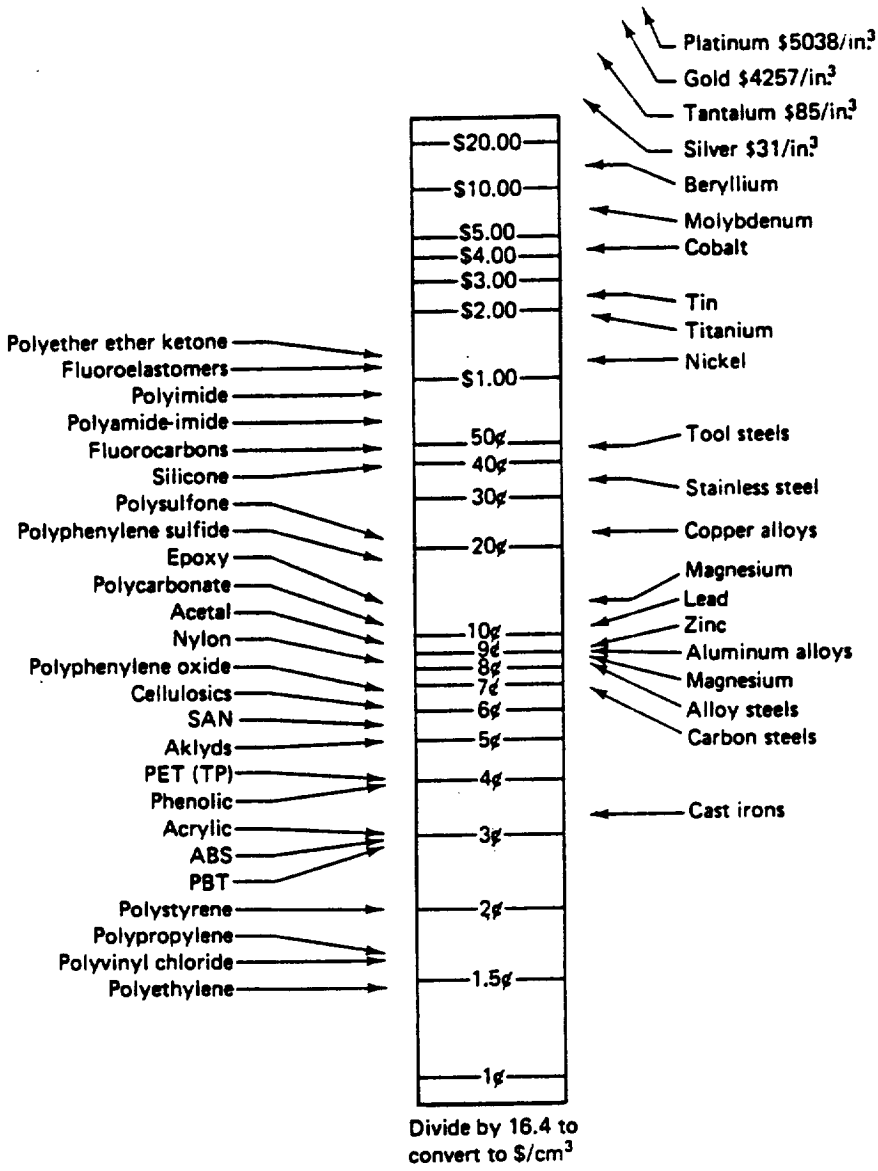

Figure 14: Costs of Common Engineering Materials per Cubic Inch

The composite is the better choice due to the strength-weight requirement. The composite material requires one-third more volume than the Al 7178-T6 but its density is almost one-half. Usage of the composite material reduces stress in the motor casing while a large weight saving can be achieved.

The cost of fabrication of the Thornel-400 epoxy composite is comparable to aluminum construction costs. The manufacturing of solid rocket motor cases does not pose any serious problems. Figure 15 shows how a filament wound motor casing can be produced. A thin epoxy matrix is applied as the filament is wound around the mold.

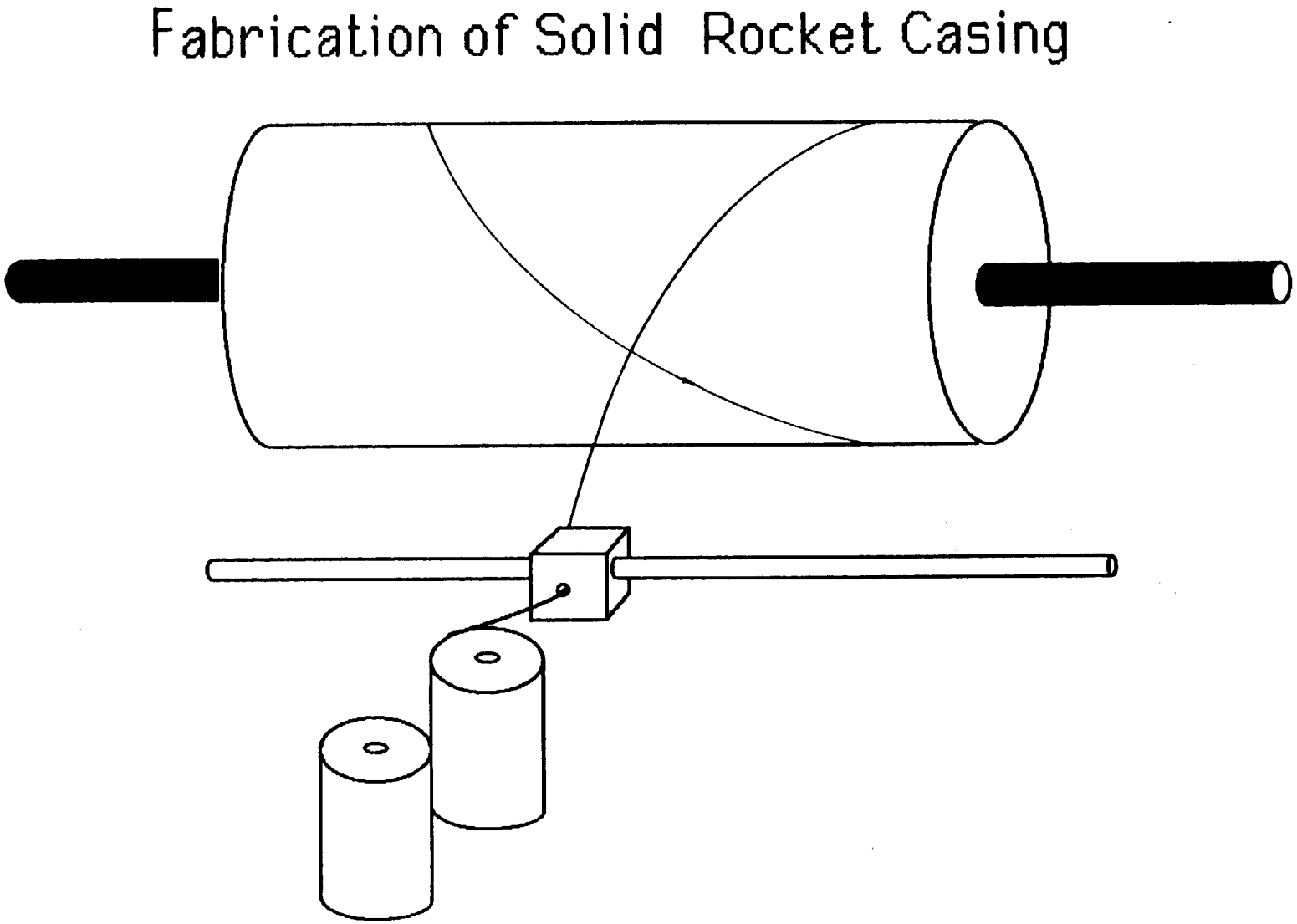

Figure 15: Fabrication of Solid Rocket Casing

Robert A. Miller
2-7-89

Structures

The structural design of the LER will be similar to normal missile designs. Large cylinder construction will be used to contain the propellant. Wall thickness will primarily depend on internal pressures and material properties. The 'short stubby' design of the LER aids in handling of the large bending moments created by LER flying at a large flight path angle and the lift due to the wing. Internal aluminum stiffeners of rings and box beams will be used to resist bending and torsional moments as well as shear strains in the material.

Figure 16 shows the stiffening options. The crossing of the graphite filaments at 45 degrees will help minimize shear by giving maximum strength in the shear plane, but crossing of 30 degrees will be used to allow for high hoop stresses and load factors, which is a large concern given the LER's trjectory.

The honeycomb, corrugated, and waffle sandwich composite designs are being pursued for the construction of the wing. Figure 17 shows the corrugated and waffle strengthening designs. This type of wing construction will keep the weight of the wing down.

Structural Booster Casing Designs

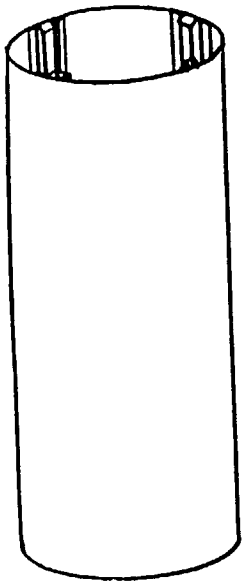

Cylindrical-Internal Stringer Reinforced

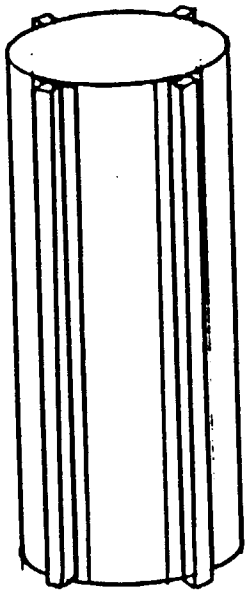

Cylindrical-External Stringer Reinforced

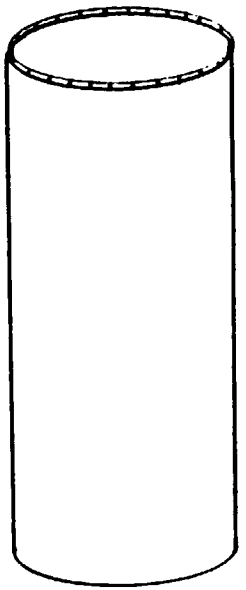

Composite Honeycomb Design

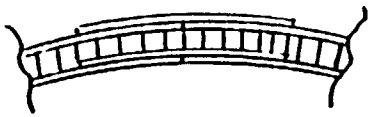

Figure 16: Solid Rocket Motor Structurals

William Jordan
2/27/89

Sandwich Composite Designs

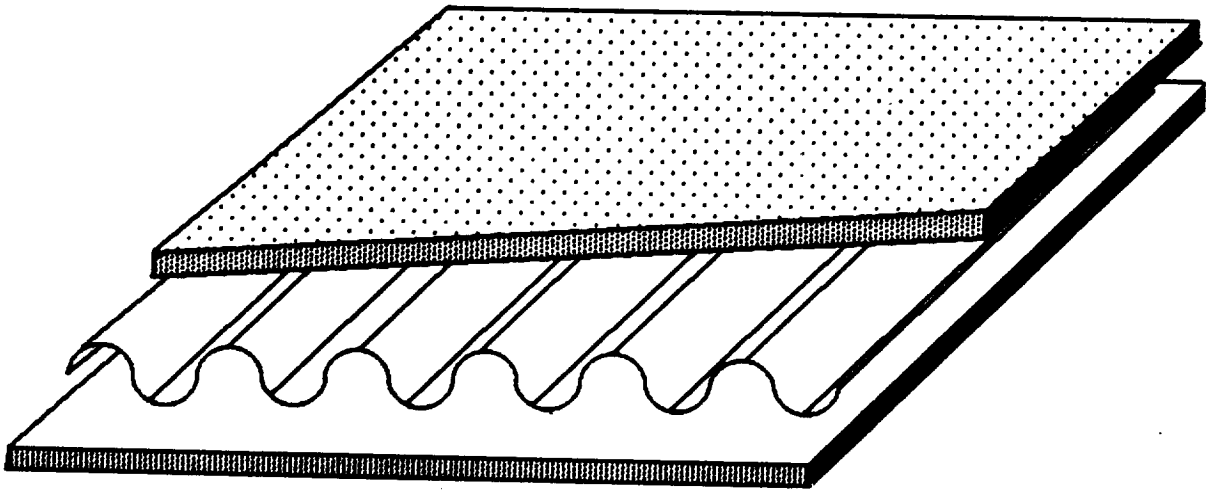

Corrugated

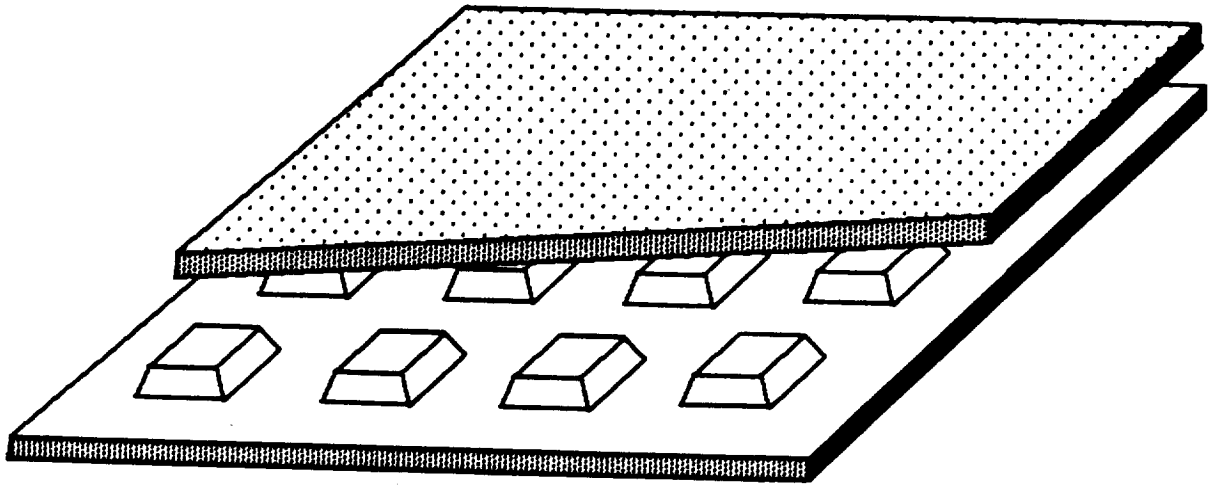

Waffle

Robert A. Miller
3-3-89

Figure 17: Composite Wing Design Options

DEVELOPMENT TIMETABLE

The LER project is expected to take three years to reach full operational capacity. The program maturity process is optimistic yet attainable. Management emphasis is placed on design evaluation to correct problems at the earliest possible moments. The following tasks will be undertaken by the LER team:

1. LER system design
2. Full scale mock-up construction
3. LER / 747 flight testing using the fully instrumented mock-up
4. Preliminary design evaluation
5. Prototype assembly
6. First launch
7. Final system evaluation
8. Production and flight of operational units.

Figure 18 is a diagram of the of the proposed task breakdown and estimated time requirements for each phase.

The system design phase includes major component design, mission analysis, and wind tunnel testing of the LER and the LER / 747 configuration. Separation from the 747 will be addressed. Once the base design has been finalized, the full scale mock-up will be constructed. This mock-up will be

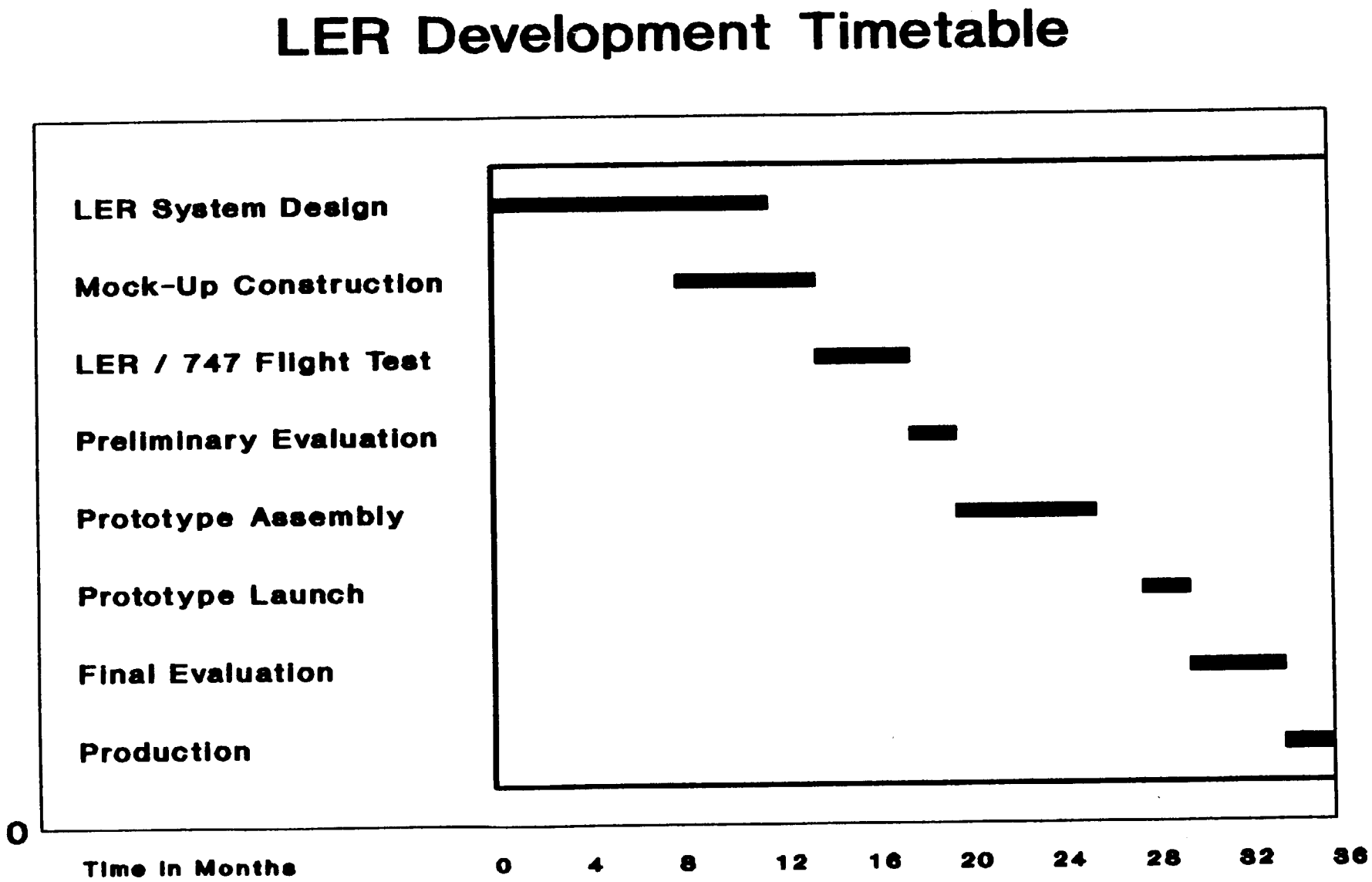

Figure 18: LER Development Timetable

instrumented for static and flight tests to directly measure flight loads and validate 747 flight behavior and ground handling techniques. Once this phase of the project is evaluated, prototype assembly will take place. After this prototype is launched (without a commercial payload), system performance will be evaluated, with any changes made before assembling operational vehicles.

Several major assemblies and components of the LER system will be contracted to other companies. These tasks include:

1. Boeing 747-100B modifications
2. Wing and tail fabrication
3. Solid rocket motor and nozzle system construction and testing.

In addition to the above list, the company tasked with solid motor construction will have design change privileges over such items as grain type, nozzle type, and fuse / inhibitor placement. Specialized knowledge in the propulsion area will save the LER team time and money. Wing and tail fabrication, along with the motor design and testing will be accomplished during the construction and testing of the full scale mock-up. The final prototype assembly, however, will not occur until after a thorough evaluation of LER / 747 configuration flight performance. Each contracted organization is responsible for creating a development timetable

complementing the main system timetable.

Although the time allotted for each phase of tasks is short, many checks exist to ensure proper design. Much emphasis is placed on testing. Above all, the LER must be a reliable system to the consumer. In the event of a failure of the mock-up or the prototype, the timetable will be sacrificed in order to produce a superior product.

DEVELOPMENT COST SUMMARY

The LER is designed to be a low cost launch vehicle. In order to pass low costs to the customer, developmental costs must be kept at a minimum. The initial design of the LER has kept price in mind at each step. Major components are devised to be inexpensive in material procurement and manufacturing. The purpose of the LER is not to advance technology, but to utilize existing technology to serve in a new fashion.

The LER development team cost is broken into parts. These sections include:

1. Development team labor
2. Office facilities
3. Airport facilities
4. 747 procurement
5. Mock-up production and procurement.

The LER core development team has overall responsiblity for the entire program until operational status is achieved. However, as mentioned before, certain aspects of the program will be tasked to other organizations. Table 12 lists the personnel desired for the core team with suggested salaries per year over a three year period.

Table 11: LER Core Development Group Pay Scale

Position	Salary / year
Lead Engineer (1)	$75,000
Senior Engineer (3)	60,000
Engineer I (4)	40,000
Technician (5)	30,000
Draftsman (4)	25,000
Clerk (2)	22,000
Co-Op Position (2)	15,600

The contracts to other organizations for design and production of components complete the LER cost analysis:

1. 747 modifications
2. Prototype wing and tail test and production
3. Prototype solid motor test and production
4. Airport maintenance crews, 747 operation.

The contracts will be awarded to the lowest bidder in a sealed bid system. The wing and motor contracts will include an option for continued production past the prototype stage.

Table 13 presents the anticipated LER system development cost based upon the lists above. The team labor costs include applicable social security and insurance payments from the employer. All costs are in 1989 dollars.

Table 12: Estimated LER Development Cost Breakdown

Item	Cost
LER Team Labor (3 yrs)	$2,645,484
Office Facilities (3 yrs)	360,000
Airport Facilities (2 yrs)	120,000
747-100B Procurement	12,000,000
Mock-Up Production	5,000,000
747-100B Modification (contract)	15,000,000
Wing & Tail Test & Prod. (contract)	4,000,000
Propulsion Test & Prod. (contract)	15,000,000
Airport, 747 Operation (contract)	2,000,000
TOTAL	**$56,125,484**

SUMMARY AND RECOMMENDATIONS

This design analysis broached the feasibility and design of the winged-air launched satellite launcher concept for medium sized payloads. Several critical design questions were addressed: Aerodynamics, Materials, Propulsion, Structures, and Trajectory Analysis. From this design analysis it appears that the LER is an engineering possibility.

A management and cost analysis was also conducted to answer the question of the economic feasibility of the LER. This report found that barring large design and production overruns that the LER is a low cost way to reach low earth orbit.

Important topics for further analysis is optimization of the trajectory, propulsion, and weight management. This study has shown how the feasibility of missiles and space transportation rests upon these subjects.

Separation from the 747 should be analyzed in great detail. Wind tunnel testing, along with more accurate wing lift approximation methods are needed. A stability and control analysis for the LER is needed.

Detailed heat transfer analysis of the nozzles and motor casings is important to future estimations of available thrust. Further study is needed to optimize grain designs for the solid motors. Thrust vectoring systems and control analysis shall be detailed.

Finally, studies must be made into such areas as failure modes for the LER, cost per launch prices, and marketing strategy. The LER is a workable concept with outstanding commercial applications. This analysis certainly indicates that additional study is warranted.

BIBLIOGRAPHY

Aviation Week & Space Technology, Volume 106, Feb. 21, 1977, page 14-15.

Aviation Week & Space Technology, Volume 106, Feb. 28, 1977, page 16-19.

Aviation Week & Space Technology, Volume 106, Feb. 14, 1977, page 12-16.

Aviation Week & Space Technology, Volume 106, March 14, 1977, page 36-39.

Aviation Week & Space Technology, Volume 128, June 6, 1988, page 14-16.

Aviation Week & Space Technology, Volume 128, June 27, 1988, page 51-53.

Aviation Week & Space Technology, Volume 128, August 22, 1988, page 84-89.

Abraham, Lewis H., Structural Design of Missile and Spacecraft, McGraw-Hill Book Company, Inc., 1962.

Bonney, E. Arthur, et al., Aerodynamics, Propulsion, Structures and Design Practice, D. Van Nostrand Company, Inc.: New York, 1956.

Budinski, Kenneth, Engineering Materials: Properties and Selection, Third Edition, Reston Publishing Co., 1988.

Chin, S. S., Missile Configuration Design, McGraw-Hill, New York, 1961.

Composite Reliability, American Society for Testing and Materials, 1975.

Covert, Eugene E., Thrust and Drag: Its Prediction and Verification, Volume 98, American Institute of Aeronautics and Astronautics, 1985.

Design of Aerodynamically Stabilized Free Rockets, U.S. Army Materials Command AMCP 706-280, Jul. 1968.

Journal Aircraft, "Aeroelastic Stability of the 747/ Orbiter", Volume 14, Number 10, Oct. 1977.

Kuethe, Arnold M. and Chow. Foundations of Aerodynamics, fourth edition. John Wiley and Sons, 1986.

Lenoe, Oplinger, and Burke, Fibrous Composites in Structural

Design, Plenum Press, New York, 1980.

Osborn, J. R., Combustion/Solid Propellants, Purdue University, 1984.

Peebles, Curtus J Br., Air-Launched Shuttle Concepts, Interplanet Soc., Volume 36, Number 4, April 1983

Richardson, Terry, Composites: A Design Guide, Industrial Press Inc., New York, 1987.

Royal Aeronautical Society Data Sheets: Aerodynamics, Vol.2.

Space Planners Guide, United States Air Force Air Force Systems Command, June 1, 1965.

Sutton, George P., Rocket Propulsion Elements, fourth edition, John Wiley & Sons, 1976.

Tsai, S. W., ed., Composite Materials: Testing and Design, ASTM Press, Philadelphia, Pennsylvania, 1979.

Wood, K. D., Aerospace Vehicle Design/Spacecraft Design, Vol.2, Johnson Publishing Co., Boulder, Colorado, 1964.

1986 Annual Book of Standards: Space Simulation; Aerospace Materials; High Modulus Fibers and Composites, ASTM, Philadelphia, Pennsylvania, 1986.